INTERFACIAL TENSION IN HYDROCARBON SYSTEMS

By

JAMES RICHARD DEAM

Bachelor of Science
University of Cincinnati
Cincinnati, Ohio
1964

Master of Science
Oklahoma State University
Stillwater, Oklahoma
1966

Submitted to the Faculty of the
Graduate College of the
Oklahoma State University
in partial fulfillment of
the requirements for
the Degree of
DOCTOR OF PHILOSOPHY
May, 1969

INTERFACIAL TENSION IN

HYDROCARBON SYSTEMS

Thesis Approved:

R. N. Maddox
Thesis Adviser

John B. West

John H. Erbar

J. R. Dorton

N. D. Durham
Dean of the Graduate College

PREFACE

Experimental interfacial tension data have been obtained for the methane-nonane, butane-decane, and methane-butane-decane systems. Data for these systems, and systems in the literature, have been used to develop and test correlation methods for hydrocarbon systems. The data and calculations have shown that interfacial tension data for hydrocarbon systems can be correlated by an excess interfacial tension concept.

I wish to express my thanks to Dr. R. N. Maddox for the guidance and advice that he has given me during this work. I would also like to thank Dr. J. H. Erbar, Dr. J. B. West, Dr. K. J. Bell, and Dr. J. R. Norton for the advice they gave as my Doctoral Advisory Committee.

I express my gratitude to the Natural Gas Processors Association for the financial and equipment support which made this work possible.

Special thanks go to my wife, Linda, for her patience and encouragement during my graduate work.

TABLE OF CONTENTS

LIST OF TABLES

LIST OF FIGURES

CHAPTER I

INTRODUCTION

The need for accurate values of interfacial tension exists in several engineering areas. For example, interfacial tension plays an important role in mass transfer and heat transfer operations. Interfacial tension studies also have importance in petroleum reservoir engineering. The author of a recent investigation of information on absorption literature concluded that the absorption of gaseous components in liquid solutions is controlled and limited by the physical properties of the gases and liquids under consideration. One of the most important physical properties appeared to be interfacial tension.

The primary objectives of this study were to measure and correlate the interfacial tension of saturated liquid mixtures of methane and heavier hydrocarbons in equilibrium with the corresponding vapor phase. Experimental measurements were to be made at temperatures and pressures that simulate absorber conditions. Therefore, experiments were to be conducted at temperatures below ambient and at pressures up to about 1500 psia. Initial experiments were to involve measurement of interfacial tension of methane

in nonane. Later stages of experimental work were to deal with ternary mixtures.

The equipment used in this study was a high-pressure pendant drop apparatus. Supporting equipment included a temperature control system, an optical system, and a pressuring system.

Experimental data were obtained for the methane-nonane binary system, the butane-decane binary system, and the methane-butane-decane ternary system. Experimental data and literature data were correlated to determine a general predictive technique for interfacial tension.

CHAPTER II

LITERATURE SURVEY

Definitions

Despite widespread information on surfaces in textbooks and elsewhere, confusion often results over distinction between the two common forms of boundary tension, surface tension and interfacial tension. Andreas and colleagues (2) defined boundary tension in general as a measure of the free energy of a fluid interface. Accordingly, they defined surface tension as the boundary tension between a liquid and a gas or vapor. They also defined interfacial tension as a measure of the free energy at a phase boundary between two incompletely miscible liquids. In contrast, Hough and workers (20) preferred to define surface tension as a measure of the specific free energy between two phases having the same composition, for example, between a pure liquid and its vapor. Similarly, they described interfacial tension as a measure of specific free energy between two phases having different composition. Thus, by Hough's definitions, interfacial tension can refer not only to a liquid-liquid interface but also to a gas-liquid interface.

In view of the more specific definitions of Hough and

the systems studied in this investigation, the convention reported by Hough was adopted.

Methods for Measuring Surface Tension

Adamson (1) has written an excellent and extensive review of various methods for measuring surface (or interfacial) tension. He includes advantages and disadvantages of the different procedures. The most commonly used methods he describes are capillary rise, drop weight, ring, maximum bubble pressure, and pendant drop.

The capillary rise method is based on the behavior of liquid in a capillary tube. Surface tension is calculated from observations of height of rise of liquid in the tube. Measurements may be made up to the critical temperature since the capillary and liquid can be sealed in a strong glass tube. For the same reason, the capillary rise method is valuable when dealing with reactive and hygroscopic substances. However, the capillary rise method is not recommended for routine use since extreme precautions must be taken. Among the disadvantages of the method are difficulties in observing the meniscus, indirect measurements of the tube diameter, meniscus correction is required, and difficulties with accurate readings when the capillary rise is small.

The drop weight method is based on the weight or volume of drops falling from a vertical tube of known size. This method is not strictly static in nature since the

method involves the enlarging and breaking of a surface. The drops must be formed slowly and premature disruption not brought about by vibration. Experience has shown that the static methods are more reliable, accurate, and reproducible than those methods of a dynamic nature. The drop weight method requires the use of correction factors. Another disadvantage is that this procedure is empirical. The apparatus must be calibrated with a fluid of known surface tension.

The ring method is founded upon the force required to pull a wire out of the liquid surface. This procedure is likewise empirical and also involves the enlarging and breaking of a surface.

Sugden (46) developed the bubble pressure method on observations of the pressures required to liberate bubbles of an inert gas from a capillary tube immersed vertically in a liquid. The bubble pressure technique may be used over a wide range of temperatures. Since a new surface is formed by each bubble, traces of impurities adhering to the capillary are soon carried away. Another advantage of this method is that it is not dependent on the contact angle.

Pendant Drop Method

The pendant drop technique for measuring surface tension was chosen for the work reported here. The method previously was not held in high esteem because of

difficulties in accurately measuring the parameters involved. With improved optical devices and better measuring techniques, the pendant drop method has become one of the most reliable methods for measuring surface tension.

Andreas and workers (2) and Niederhauser and Bartell (28) have cited a list of advantages of the pendant drop method over other methods. The pendant drop method is an absolute method; that is, it has been subjected to complete, quantitative mathematical analysis. Thus, this method does not require calibration with a liquid of known surface tension. A small amount of liquid may be used since only a pendant drop is measured. Diameters of relatively large drops are measured directly; thus, the method is capable of yielding results of a higher degree of accuracy than other methods. The pendant drop method is easily adapted to measurements under high pressure, and the photograph of the drop serves as a permanent record for future reference. The drop surface is not disturbed prior to or after measurement. Other advantages include its use for highly viscous liquids and its applicability to both surface and interfacial tension. Boundary tensions of any magnitude can be observed. In addition, the results do not depend on the contact angle.

The equation of Laplace and Young (1) forms the basis for the pendant drop method:

$$P = \gamma\left(\frac{1}{R} + \frac{1}{R'}\right). \qquad (1)$$

Equation (1) shows that the pressure difference on two sides of a curved interface between two fluids is the product of the boundary tension and a mean radius of curvature. For figures of revolution (49), for example the drop in Figure 1, the equation for pressure difference across an interface is

$$P = (d_L - d_V)gz + \frac{2\gamma}{b}. \tag{2}$$

Combining Equations (1) and (2) after substitution for the radii of curvature yields

$$\frac{2}{b} + \frac{gz(d_L - d_V)}{\gamma} = \frac{\sin\varphi}{x} + \frac{1}{\rho}. \tag{3}$$

Defining β as

$$\beta = \frac{-gb^2(d_L - d_V)}{\gamma} \tag{4}$$

and substituting into Equation (3) yields

$$\frac{1}{\rho} + \frac{\sin\varphi}{x} = \frac{2}{b} + \frac{\beta z}{b^2}. \tag{5}$$

Using b as unit length, or equivalently defining drop co-ordinates as

$$Z = \frac{z}{b}$$

$$X = \frac{x}{b} \tag{6}$$

and introducing the equation for the radius of curvature,

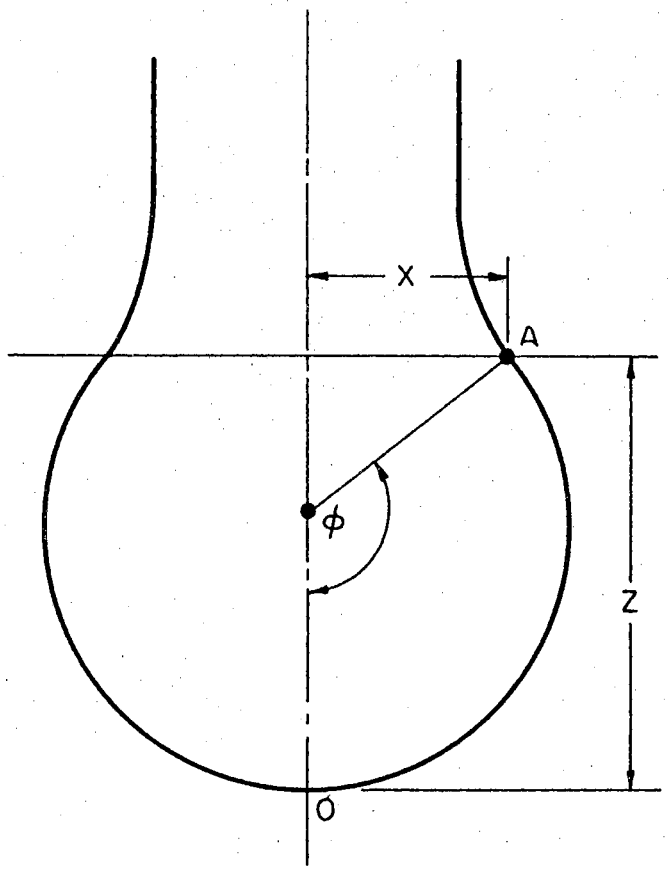

Figure 1. Profile of a Pendant Drop

$$\rho = \frac{\left[1 + \left(\frac{dz}{dx}\right)^2\right]^{3/2}}{\frac{d^2 z}{dx^2}} \tag{7}$$

substitution into Equation (5) gives

$$Z'' + \frac{Z'}{X}[1 + (Z')^2] = [2 - \beta Z][1 + (Z')^2]^{3/2}. \tag{8}$$

Equation (8) is a second-order, non-linear partial differential equation for which no analytical solution is known. However, a solution for the surface tension may be obtained by combining Equation (5) with the equations describing the profile of the drop

$$\frac{1}{\rho} = \frac{d\varphi}{ds}$$

$$\frac{dx}{ds} = \cos\varphi \tag{9}$$

$$\frac{dz}{ds} = \sin\varphi.$$

Two appropriate diameters of the drop, illustrated in Figure 2, are defined to facilitate the solution of Equations (4), (5), and (9). A shape factor is defined as

$$S = \frac{d_s}{d_e} \tag{10}$$

where d_e is the equatorial diameter, corresponding to the angle $\varphi = 90^\circ$ on the drop profile, and d_s is a selected plane diameter at a distance d_e from the vertex of the drop. Since b, the radius of curvature of the drop at the

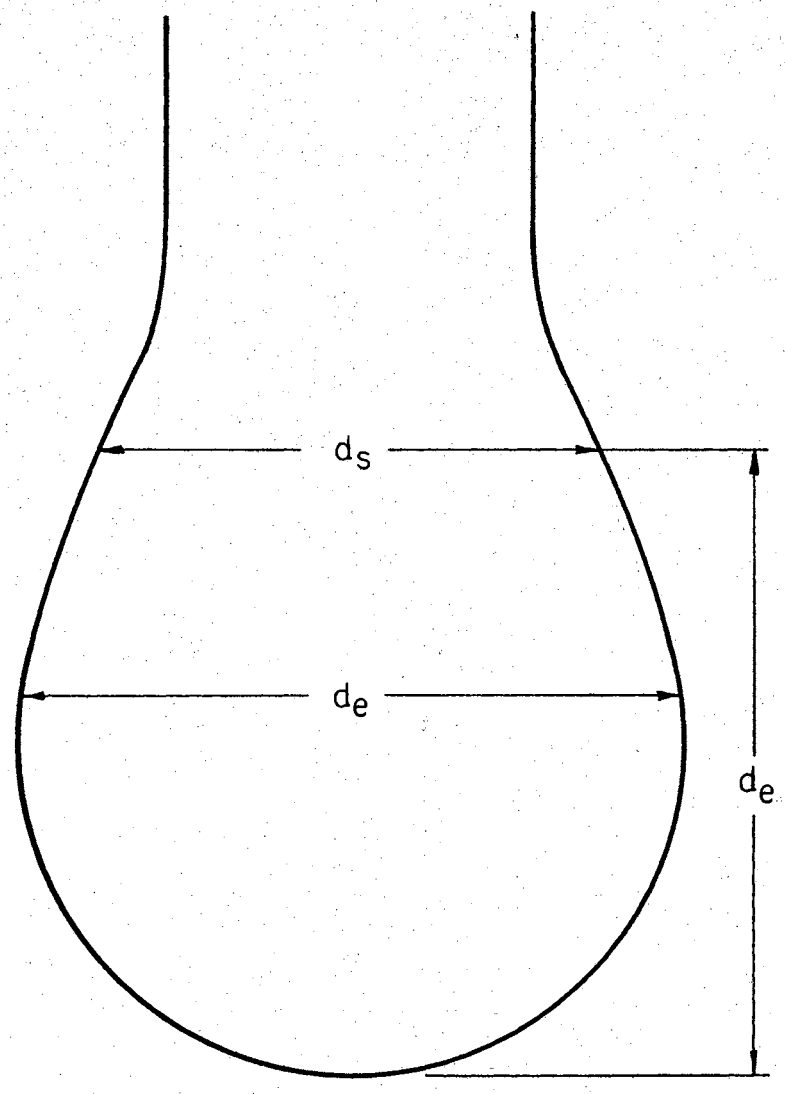

Figure 2. Drop Diameters for Pendant Drop Method

origin, and β cannot be measured precisely or quickly from a photograph of the drop, a shape dependent parameter is defined as

$$\frac{1}{H} = -\frac{1}{\beta(de/b)^2}. \tag{11}$$

Substitution of Equation (11) into Equation (4) gives the equation for calculation of surface (or interfacial) tension

$$\gamma = \frac{g(d_L - d_V)\, d_e^2}{H}. \tag{12}$$

A problem remains to obtain a numerical evaluation of the function 1/H versus S. The solution requires selection of various values of β, integration of the profile equations to find d_e and d_s, and calculation of the corresponding S and 1/H values. Subsequently, a tabulation of 1/H versus S is established by use of an interpolation formula.

Several shape factor tabulations appear in the literature. Andreas and workers (2) doubted the accuracy of previous numerical integration techniques and evaluated the shape function empirically. They measured diameters of a large number of drops of water from various-sized dropper tips. However, calculations from such a table are relative to the accuracy of data for the surface tension of water.

Fordham (13) recognized that the profile equations

could be solved accurately by the Bashforth-Adams (4) integration formula. He constructed a shape factor table for S values from 0.66 to 1.0. At the same time, Niederhauser and Bartell (28) independently calculated shape factors for S values over the same range. Their values agreed closely with those of Fordham. Niederhauser and Bartell showed a systematic error in the tables of Andreas of as much as 1.4 per cent. Later, Mills (26) also used the Bashforth-Adams formula to derive S values from 0.46 to 0.6. Recently, Stauffer (44) used an integration by reiterated approximations to construct a table for S from 0.30 to 0.67. His results agreed with those of Mills.

The author used a method of successive approximations in this work for shape factor evaluation to check the results of the workers above. The resulting shape factors agreed well with those derived through use of the Bashforth-Adams and reiterated approximation techniques described above.

Summarizing, the pendant drop calculations can be made as accurate as desired by carrying out the shape factor integration to a small error. The pendant drop method is absolute, requiring no calibration. Measurement of two diameters, d_e and d_s, provides a shape factor S, from which the corresponding value of 1/H may be found. Equation (12) is used to calculate the surface (or interfacial) tension.

Theory and Correlations

Gambill (15) has reviewed the early developments proposed for estimating surface tension. In 1886, Eotvos (10) correlated surface tension with temperature to obtain

$$\gamma (MV_L)^{2/3} = k(T_c - T). \tag{13}$$

Ramsay and Shields (33) modified the Eotvos equation to correspond more closely to their data at temperatures not near the critical temperature

$$\gamma (MV_L)^{2/3} = k(T_c - T - \delta). \tag{14}$$

They found that δ was usually six degrees. Later, Katayama (15) further modified the Eotvos equation by including the vapor density

$$\gamma (M/\Delta\rho)^{2/3} = k(T_c - T). \tag{15}$$

Inclusion of the vapor density improved the previous correlations since the new equation applied to a wider temperature range. These correlations are based on the Eotvos constant, k, which is approximately 2.12 for normal (unassociated and nonpolar) liquids. However, Gambill reported that k varies from at least 1.5 to 2.6 for other liquids. For this reason, these correlations are not acceptable except for a narrowly defined group of liquids.

In 1894 van der Waals (48) proposed a correlation for surface tension with reduced temperature

$$\gamma = K_1 T_c V_c^{-2/3}(1 - T_r)^n$$

$$= K_2 T_c^{1/3} P_c^{2/3}(1 - T_r)^n$$

$$= \gamma_o(1 - T_r)^n. \qquad (16)$$

van der Waals proposed that K_1, K_2, and n are universal constants for all liquids. He gave the value of the exponent as 1.5. Later, Ferguson (12) confirmed van der Waals' equation but gave the exponent as 1.2.

Ferguson also combined the Katayama and van der Waals equations to arrive at the equation

$$\gamma^{1/4} = C \cdot \Delta\rho \qquad (17)$$

Ferguson reported that the constant C was essentially temperature independent. Macleod (25) reported the same relationship on empirical grounds from the Ramsay-Shields data.

Sugden (47) proposed the parachor from consideration of, and as an extension to, the Ferguson and Macleod relation

$$[P] = \frac{M\gamma^{1/4}}{\Delta\rho}. \qquad (18)$$

Sudgen suggested that the parachor is an additive property. He constructed the first group contribution tabulation making the parachor an additive function of the atoms and groups in the molecule. He also found that the parachor

was nearly temperature independent. Only small deviations were found among substances that associate.

Recently, Quayle (30) has published a more detailed tabulation of atom and group contributions and parachors of pure substances. An alternative approach (19), but less accurate, has been to relate the parachor to the Lennard-Jones potential parameters.

Several arguments have been offered on the foundations of the parachor. Sugden suggested that the parachor is a comparison of molecular volumes at constant surface tension. He proposed that the parachor is a true measure of the molecular volume when the parachor is compared with the critical volume and the mean collision area. He further argued that the equations of Laplace show that the ratio of surface tension to cohesion is of the same order of magnitude as the range of molecular forces. This ratio is proportional to the molecular diameter which is of the same order as the range of action of these forces.

Lowry (23) proposed that the influence of temperature on specific and molecular volumes can be eliminated completely if the density difference is divided by surface tension to the one-fourth power

$$\frac{\Delta \rho}{\gamma^{1/4}} = \text{constant}. \qquad (19)$$

The function

$$\frac{M\gamma^{1/4}}{d_L - d_V} = [P],$$

Lowry wrote, is in fact a molecular volume, M/d_L, which has been corrected with the surface tension for the overwhelming influence of internal pressure of the liquid.

Reilly and Rae (37) argued that physical foundations of the parachor were rather weak. From a molecular similarity concept they derived a relation for the parachor

$$[P] = 0.41\ T_c^{1/4}\ V_c^{5/6}. \qquad (20)$$

They stated that the parachor does not have the dimensions of volume. They also showed that the constancy of the ratio of $[P]/V_c$ as proposed by Sugden is more than doubtful for many substances.

Fowler (14) theoretically deduced the Sugden parachor relationship and the Macleod equation. He developed a statistical theory for the surface tension of a liquid in contact with its own vapor. However, Fowler could give no reason for expecting that Macleod's equation should hold over fairly wide ranges of temperature.

Recent work on the parachor relation has been aimed at determining the value of the exponent. Wright (53) has criticized the use of the exponent 4. He found, from a regression analysis of experimental data at various temperatures, that the best value of the exponent varies from 3.5 to 4.5 for different materials. However, Wright neither suggested nor attempted a general correlation for the exponent.

A different approach for the correlation of surface tension of pure components has been proposed by Brock and Bird (8). As can be seen from the van der Waals equation, Equation (16), the ratio of $\gamma/T_c^{1/3} P_c^{2/3}$ is dimensionless except for a numerical constant depending on the choice of units employed. Brock and Bird derived the equation

$$\frac{\gamma}{T_c^{1/3} P_c^{2/3}} = (0.133 \alpha_c - 0.281)(1 - T_r)^{11/9} \qquad (21)$$

α_c is the Riedel critical parameter (39), the slope of the vapor pressure curve at the critical point. The relationship was tested for 84 widely different non-polar organic compounds and permanent gases and gave an average deviation of about three per cent.

Few mixture correlations have been described in the literature. In general, the existing correlations describe ideal or nearly ideal solution behavior.

Stakhorsky, as reported by Gambill (15), postulated that surface tension is proportional to internal pressure and derived the equation

$$\gamma = \frac{\gamma_1 \gamma_2}{x_1 \gamma_1 + x_2 \gamma_2}. \qquad (22)$$

Equation (22) is valid only at low pressure. Bowden and Butler (6) later investigated Stakhorsky's equation. They found Equation (22) to hold well when the critical temperatures of the pure components do not differ greatly.

Hammick and Andrew (17) found that surface tension of

mixtures could be calculated from

$$\gamma^{1/4} = \frac{[P]}{M} \Delta\rho \qquad (23)$$

if M and [P] were molal-average quantities. However, this approach is unsatisfactory at elevated pressures or when mixtures are associated, dissociated, or polar.

Experimental Data

Weinaug and Katz (52) extended the work of Hammick and Andrew to include the vapor phase at elevated pressures

$$\gamma^{1/4} = \frac{d_L}{M_L} \Sigma\, x_i[P_i] - \frac{d_V}{M_V} \Sigma\, y_i[P_i]. \qquad (24)$$

They experimentally measured the interfacial tension of the methane-propane system and found excellent agreement with interfacial tension values calculated from Equation (24).

Reno and Katz (38) employed the same relationship to correlate their experimental nitrogen-butane and nitrogen-heptane interfacial tension data. They calculated the parachor for nitrogen dissolved in butane to be 60, which is in agreement with the pure component value for nitrogen. However, they calculated a parachor for nitrogen in heptane of 41. They concluded that the parachor for nitrogen may not have a constant value when nitrogen is a component in various mixtures.

Recent interfacial tension work has been conducted

for systems at temperatures and pressures close to the critical region. Stegemeier and Hough (45) investigated the methane-pentane and the methane-decane systems at temperatures from 100° to 200° F and pressures from 500 to 5300 psia. Pennington and Hough (29) measured interfacial tension in the methane-butane binary system at 100°-190° F and 1300-1900 psia. Brauer and Hough (7) observed interfacial tension in the carbon dioxide-butane system at 100°-175° F and 650-1200 psia. Hough and colleagues chose to correlate their results using the Weinaug-Katz mixture rule, but with different exponent and parachor values. They based their exponent choice on Guggenheim's (16) density difference observations which give rise to an exponent of 3/11 instead of the usual 1/4 for the interfacial tension equation.

Recently, Warren (50) measured interfacial tension values for the ethylene-heptane and the methane-n-heptane systems. Experimental data were collected at temperatures from 100° to 310° F and pressures from 200 psia to close to the critical region. These data and the methane-propane, methane-butane, methane-pentane, methane-decane, and butane-carbon dioxide systems were likewise correlated with the Weinaug-Katz relationship having the exponent 3/11. The parachor value of each component was found by regression analysis and compared with the pure component values reported by Sugden and Weinaug and Katz. A modified form of the pure-component equation of Sugden

$$\gamma = B(d_L - d_V)^E \qquad (25)$$

was used to analyze the seven binary systems. However, Warren could not draw any firm conclusions from this analysis.

In summary, most of the experimental data reported in the literature was measured at temperatures of 100° F or greater. In addition, experimental investigations were limited to binary systems. Attempts to accurately correlate interfacial tension data were only moderately successful.

For these reasons, the experimental work reported in this study was undertaken. Primary considerations were to make measurements of interfacial tension at temperatures below ambient and for ternary systems.

CHAPTER III

EXPERIMENTAL APPARATUS

A schematic diagram of the experimental apparatus used in this investigation is shown in Figure 3. The basic elements are a high-pressure cell, a sample introduction system, a temperature control system, and an optical system. Other components include a pressuring system and a liquid sampling system.

The high-pressure cell was a stainless steel chamber approximately three inches in outside diameter and four inches long. The internal volume of the cell was fourteen cubic centimeters. Each end of the cell was fitted with an optical quartz lens three-fourths inches in diameter. High-pressure connections to the cell were provided for pressuring the cell with gas and for introducing the liquid sample.

The drop forming apparatus, shown in Figure 4, was used to introduce the liquid sample into the cell. A vernier screw driving a piston with an O-ring seal forced liquid from the reservoir into a six-inch length of stainless steel capillary having an inside diameter of 0.087 inch. A straight-through ball valve, having an orifice the same size as the capillary, was inserted into the

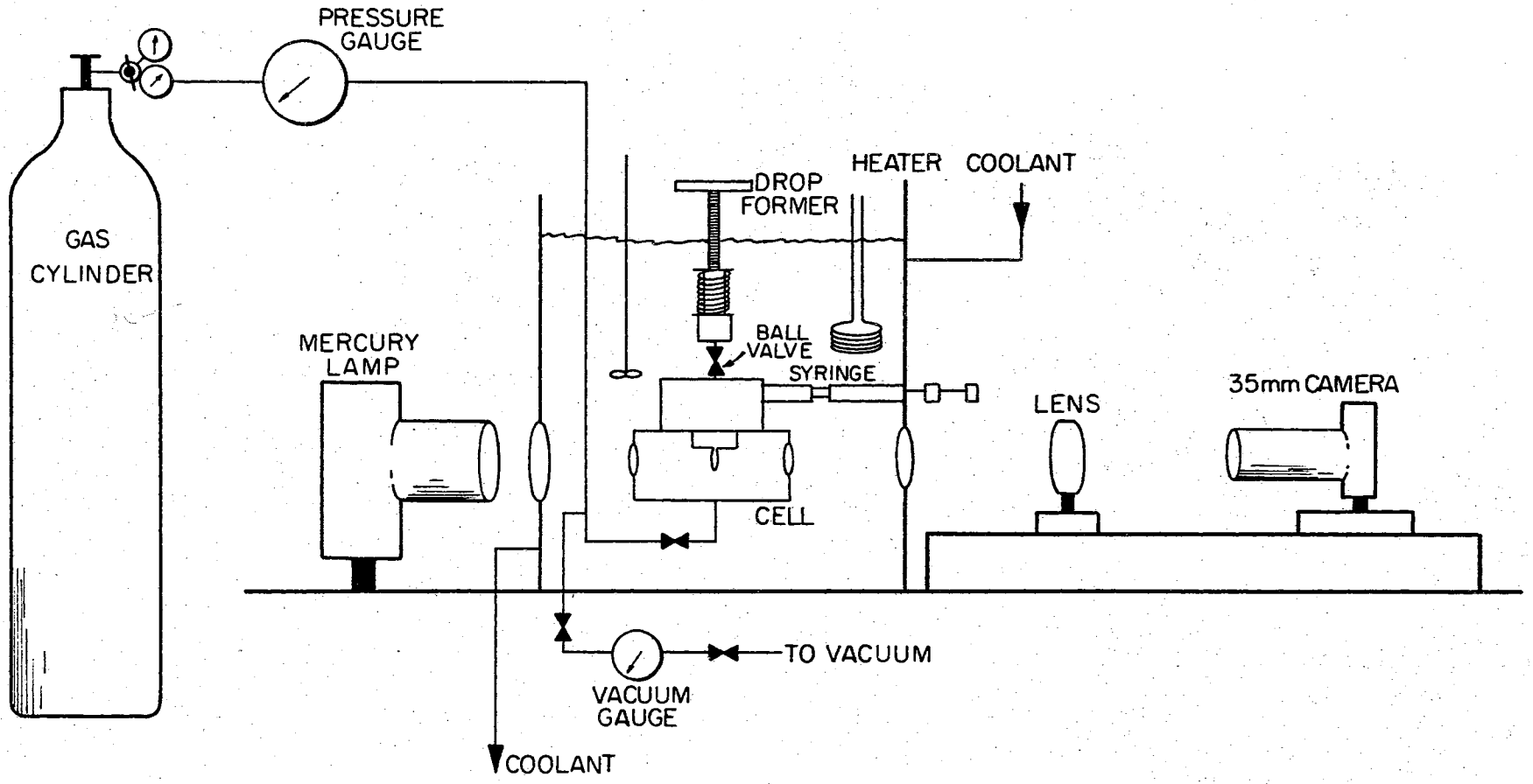

Figure 3. Experimental Apparatus

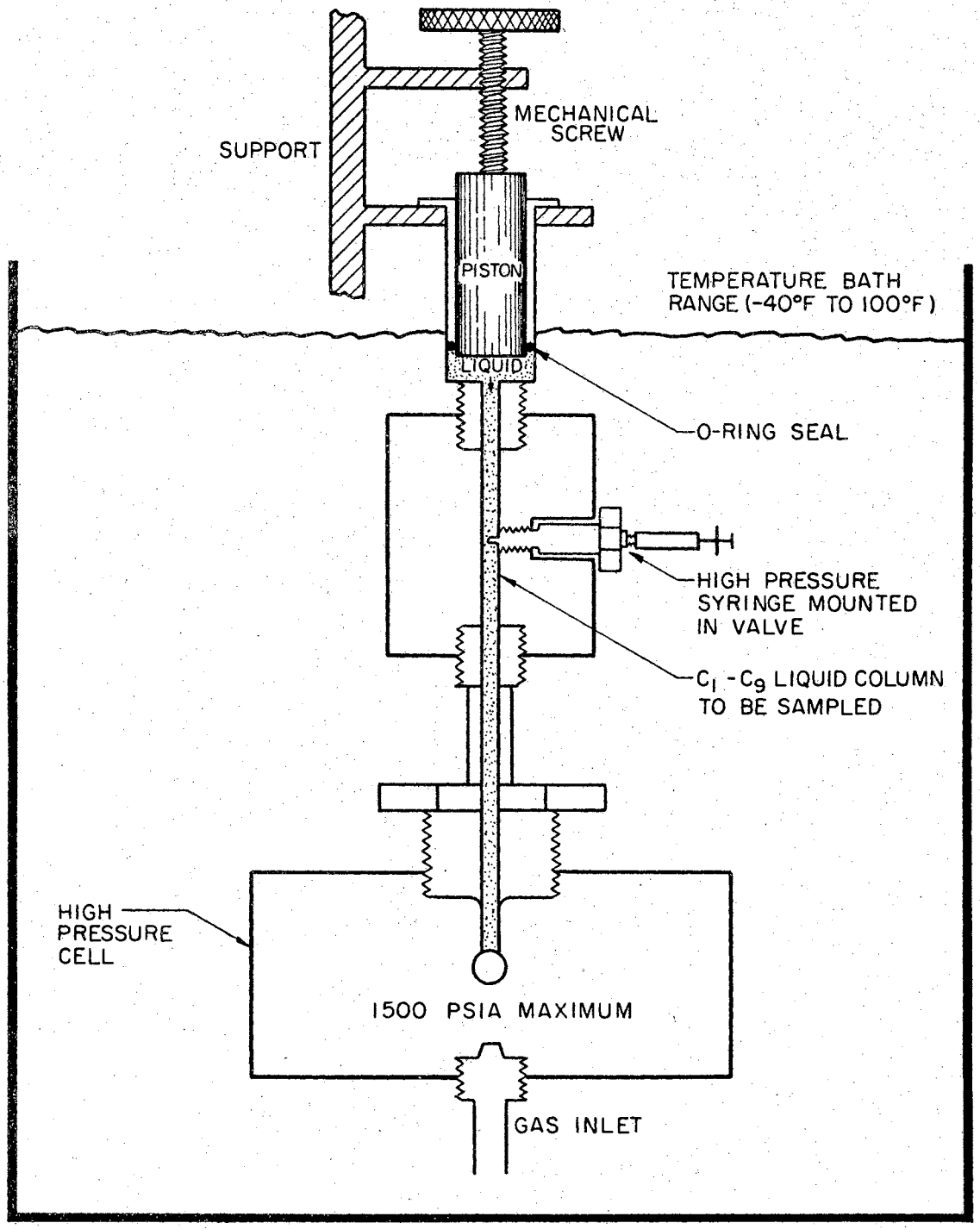

Figure 4. Drop-Forming Apparatus and Liquid Sampling System

capillary line to separate the liquid reservoir from the cell. A Yale Number 15 stainless steel capillary tip (.1836 inch inside diameter) was attached to the pressure fitting inside the cell and was visible from the cell windows. Care was taken to keep the volume of the capillary and sample system as small as possible, so that a minimum amount of hydrocarbon could be used.

At various times, a liquid sampling system, illustrated in Figure 4, was inserted into the capillary line to withdraw liquid samples for analysis. Samples were removed by a Precision Sampling Corporation sampling valve and high-pressure syringe. Samples were analyzed on a Varian-Aerograph Flame Ionization Series 1200 Chromatograph. To facilitate composition analysis, a Perkin-Elmer D2 digital integrator was used to convert the chromatograph voltage response to a digital response.

The cell was pressured with gas directly from the pressure cylinder. The system pressure was registered on Heise and Marsh pressure gauges.

The entire cell and drop forming assembly were contained in a constant temperature bath capable of maintaining temperatures between -40° F and 120° F. The bath was insulated with one inch of magnesia packing between the walls and one inch of fiberglass on the outside. Bath control was provided to 0.1° F by a Thermistemp Model 63 temperature controller. Heat was supplied with a 300-watt immersion heater. Refrigeration was provided by a locally

fabricated compression-type refrigeration unit charged with Freon 22.

The principal components of the optical system were the light source, the camera, and the optical comparator. A Cenco 100-watt high-pressure mercury arc light was placed at one window of the cell and a Nikon Model F 35mm single-lens reflex camera at the other window. The photograph was recorded on Kodak extreme resolution panchromatic film. To facilitate measurement, the droplets were projected on a Gaertner 925-AP optical comparator and a Vanguard Model C-11D motion analyzer, which give 30X and 16X magnification, respectively.

The liquid hydrocarbons used in this study were research grade and the hydrocarbon gases were instrument grade, obtained from Phillips Petroleum Company. The specifications on the hydrocarbons are the following:

	mole per cent	
research-grade nonane	99.68	
	0.32	iso-nonanes
research-grade decane	99.49	
	0.51	iso-decanes
instrument-grade butane	99.55	
	0.40	iso-butane
	0.05	propane
instrument-grade methane	99.29	
	0.60	nitrogen
	20	ppm max. oxygen
	10	ppm max. water

CHAPTER IV

EXPERIMENTAL PROCEDURE

An experimental run consisted of determination of interfacial tension at an isotherm for various pressures.

Before an experimental run, the drop-forming apparatus and the cell were cleaned. An initial ultrasonic cleaning with distilled water was followed with a hydrocarbon liquid wash. The equipment was allowed to drain, and filtered air was passed through for drying.

Two-Component Systems

In order to start a run, the drop-forming apparatus and the cell were assembled and immersed in the temperature bath. The entire system was made leak-free at a pressure higher than the pressure values for the run. The temperature bath was adjusted to the specified temperature and the entire system brought to temperature equilibrium. The system was evacuated to approximately five microns, and the hydrocarbon gas was introduced at a pressure slightly greater than atmospheric pressure. The valve in the capillary was opened, and the piston was withdrawn to the top of the reservoir. The hydrocarbon liquid was injected into the reservoir from a syringe. Every effort

was made to use the minimum amount of hydrocarbon liquid, usually not more than eight drops. The gas was allowed to bubble through the liquid for a few minutes; then the piston was pushed down into the reservoir and the capillary valve was closed. The gas pressure in the cell was raised to the desired level.

After allowing the system to again reach thermal equilibrium, the capillary valve was opened and the mechanical screw used to force a droplet of liquid to the end of the capillary. Liquid mixing was accomplished by continuously exposing new liquid surface to the vapor. Mixing was aided by alternately retracting the piston to suck liquid back into the reservoir and then forcing liquid back down the capillary. Sufficient time, at least thirty minutes, was allowed for the system to reach pressure and mass transfer equilibrium. When convective currents in the undisturbed droplet had damped and the drop became pendant, at least three photographs were taken. Vibrations were reduced with shock pads and by turning off all motors. Vibrations resulting from normal traffic in the building usually necessitated data taking during evenings and on weekends.

After the photographs were taken, the pressure was raised to the next desired value. The procedure outlined above was repeated.

Extreme care was taken to assure that the drop formed on the end of the capillary was truly pendant. Figure 5

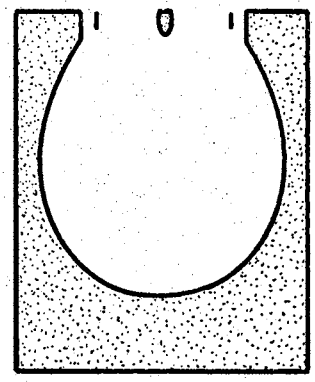

(A)

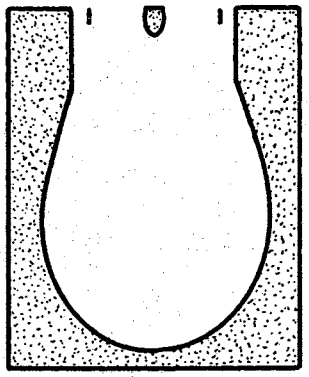

(B)

Figure 5. Drops Suspended From a Capillary Tip

shows examples of two droplets. Figure 5A shows a droplet that is not pendant. Figure 5B is a droplet that is pendant, just before being detached from the capillary. Considerable error in interfacial tension measurement can be caused by an improperly formed drop on the capillary tip.

An interesting phenomenon was observed as the droplets were formed on the capillary tip. As the gas dissolved in the liquid, the liquid droplet would disappear back up the capillary passage. This movement was partially attributed to mass transfer between the gas and the liquid. When a pendant drop remained on the capillary tip, mass transfer equilibrium between the gas phase and liquid phase was assumed to have been established.

After the photographs were developed and measurements made, the measurements of each drop were checked against the capillary-tip-size correlation of Niederhauser and Bartell (28) to make certain that the droplets were in the stable and pendant region.

Three-Component Systems

The preliminary procedure for the methane-n-butane-n-decane system was the same as for binary systems. Decane was injected into the reservoir and butane was bubbled through the liquid. The capillary valve was closed and the piston lowered into the reservoir. The cell was evacuated and then raised to the butane gas pressure to

achieve the desired butane-decane liquid composition. The valve was then opened and the pressure set at the bubble point pressure. The liquid was mixed by the agitation procedure described before.

After photographs of the butane-decane binary were taken, methane was added to bring the system pressure to the bubble point pressure required for the desired liquid composition.

Experimental Liquid Analysis

In the early phase of experimental work, sampling techniques were used to analyze the liquid phase in the system. The reasons were to determine liquid composition and liquid density, since liquid density enters directly into the equation for interfacial tension. Since liquid density data for the methane-nonane system were not available in the literature at the time this investigation was started, a reliable means for finding the density was necessary.

A chromatographic technique was attempted for determining mixture liquid composition and density. By this method, pure-component samples of various known volumes of the substances comprising the mixture were injected into the chromatograph. The resulting responses from the integrator were used to construct pure-component calibration curves (weight versus response) for each component.

To determine the density and composition of the

mixture, a known and fixed-volume sample was analyzed, and the response of each component was obtained. The weight of each component was determined from the corresponding pure-component calibration curve. The density was calculated from the sample weight and volume thus obtained.

The sampling system first tried was the Pan American Petroleum Corporation technique discussed by Yarborough (54). The sampling valve shown in Figure 6 was connected to the capillary line between the liquid reservoir and the high-pressure cell. The liquid stream passed through the channel in the body of the high-pressure valve. A sample was trapped in the cavity and sealed off by turning the valve stem into the seat. With the sample sealed off in the cavity, the valve was disconnected from the capillary and was inserted into the carrier gas line leading to the chromatograph. With the stem still in the closed position, the carrier gas was passed through the valve channel and around the stem to remove air and any remaining liquid from the sampling valve. The valve stem was then opened to allow the carrier gas to sweep the sample from the cavity.

Considerable difficulty was experienced with this technique. The method was rather awkward since the sample valve had to be repeatedly removed from and installed in both the interfacial tension apparatus and the chromatograph equipment. Also experience showed that always no more than a portion, and sometimes none, of the liquid

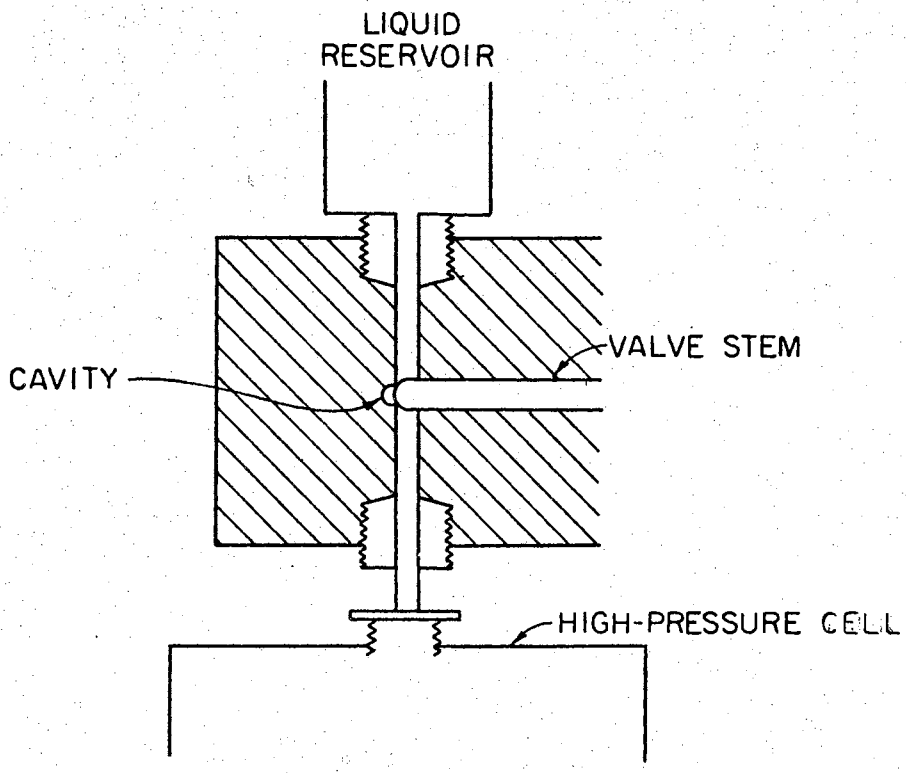

Figure 6. Pan American Type Sampling Valve

from the cavity was swept into the chromatograph. Also, the sample size delivered to the chromatograph was not reproducible. Heating the sampling valve to vaporize the sample showed no substantial improvement.

Since reliable sampling could not be obtained with the Pan American apparatus, another method for liquid sampling was investigated. A Precision Sampling Corporation valve and high-pressure syringe, illustrated in Figure 7, were fitted into a sampling adapter which was installed in the capillary line. Figure 4 shows the position of the sampling system relative to the interfacial tension apparatus. Prior to making a run, the sample valve was opened and the system was evacuated to remove air from the sampling system. Before sampling, the liquid in the system was mixed by the procedure discussed earlier. Then the sample valve was opened. Extreme care was required to obtain the desired amount of liquid sample. The valve was then closed to seal off the system pressure, and the liquid in the syringe was injected into the chromatograph. Samples could be taken in this manner without shutting down the system or disconnecting the apparatus.

During the 76° F isothermal run for the methane-nonane system, liquid samples were withdrawn from the system and analyzed for composition to determine if mass transfer equilibrium between the liquid and vapor phases had been established. Table I shows the comparison between

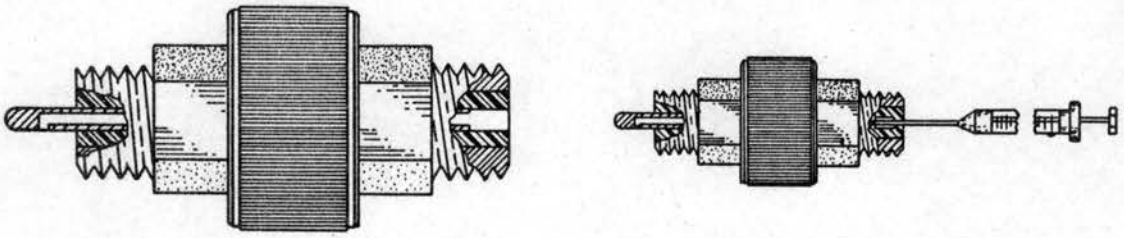

Figure 7. Precision Sampling Corporation High-Pressure Valve and Syringe

TABLE I

COMPARISON OF LIQUID COMPOSITIONS FOR METHANE-NONANE SYSTEM

Temp, °F	P, psia	Methane Mole Fraction	
		This Work	Shipman and Kohn (42)
76	150	.049	.051
		.048	
		.119	
		.176	
		.164	
		.225	
		.139	
76	300	.110	.099
		.163	
		.080	
		.198	
		.254	
76	600	.168	.183
		.354	
		.230	
		.139	

experimental liquid-phase compositions from this study and literature composition data.

In general, the sampling technique was very undependable, since full and reproducible liquid samples were difficult to obtain with the apparatus. Nearly all of the samples indicated a large amount of methane, showing that partially gas and liquid samples were obtained. In view of these difficulties, the sampling system was abandoned for the remainder of the runs.

CHAPTER V

EXPERIMENTAL RESULTS

The first experimental data were taken at ambient temperatures and at one atmosphere pressure for nonane in an air atmosphere and nonane in a methane atmosphere. These data are shown in Table II.

Table III and Figures 8, 9, and 10 show the experimental interfacial tension data taken on the methane-nonane system in this investigation. Isotherms were run at 76° F, 30° F, -10° F, and -30° F at pressures ranging from atmospheric to approximately 1500 psia. All data are for saturated liquid mixtures of methane and nonane in equilibrium with the corresponding vapor phase at experimental conditions. Interfacial tension values were generated from phase densities and experimentally-determined drop diameters through the use of Equation (12).

Experimental interfacial tension data for the butane-decane binary and the methane-n-butane-n-decane ternary are presented in Tables IV and V and Figures 11, 12, and 13. Isotherms were run at 40° and 100° F at pressures from 3 to 34 psia for the butane-decane binary and at pressures from 300 to 1150 psia for the ternary system. All of the data are for saturated liquid mixtures

TABLE II

EXPERIMENTAL DATA AT ATMOSPHERIC PRESSURE

Temperature, °F	Atmosphere	Surface Tension, dynes/cm.
77	air	22.86 21.98 22.21
77	methane	22.10 22.17 22.05

TABLE III

EXPERIMENTAL INTERFACIAL TENSION OF METHANE-NONANE SYSTEM

T = 76°F			T = 30°F			T = -10°F			T = -30°F		
Pressure psia	Interfacial Tension dynes/cm	Avg. Value	Pressure psia	Interfacial Tension dynes/cm	Avg. Value	Pressure psia	Interfacial Tension dynes/cm	Avg. Value	Pressure psia	Interfacial Tension dynes/cm	Avg. Value
15 (air)	22.71	22.76	15 (air)	25.15	25.25	140	25.32	25.05	147	24.60	24.45
	22.74			25.29			24.94			24.31	
	22.79			25.30			24.89				
	22.82								285	21.10	21.73
	22.74		15	24.66	24.37	310	21.15	21.79		21.67	
				24.07			22.79			22.42	
75	21.94	21.77					21.46				
	21.79		150	23.47	22.95		21.74		590	15.99	16.38
	21.50			22.44						15.99	
	21.87					598	16.08	15.91		17.17	
			300	19.27	19.27		15.31				
150	20.63	20.58					15.92		1025	10.27	10.41
	20.62		600	16.33	16.28		16.32			10.41	
	20.50			16.23						10.56	
	20.58					890	12.27	12.17		10.40	
			900	13.68	13.68		12.02				
300	18.93	18.93		13.69			12.32				
							12.06				
			1175	10.53	10.48						
				10.56		1190	9.28	9.27			
				10.36			9.26				
			1315	9.22							
				9.13	9.30						
				9.36							
				9.48							
			1475	8.33	8.26						
				8.24							
				8.20							

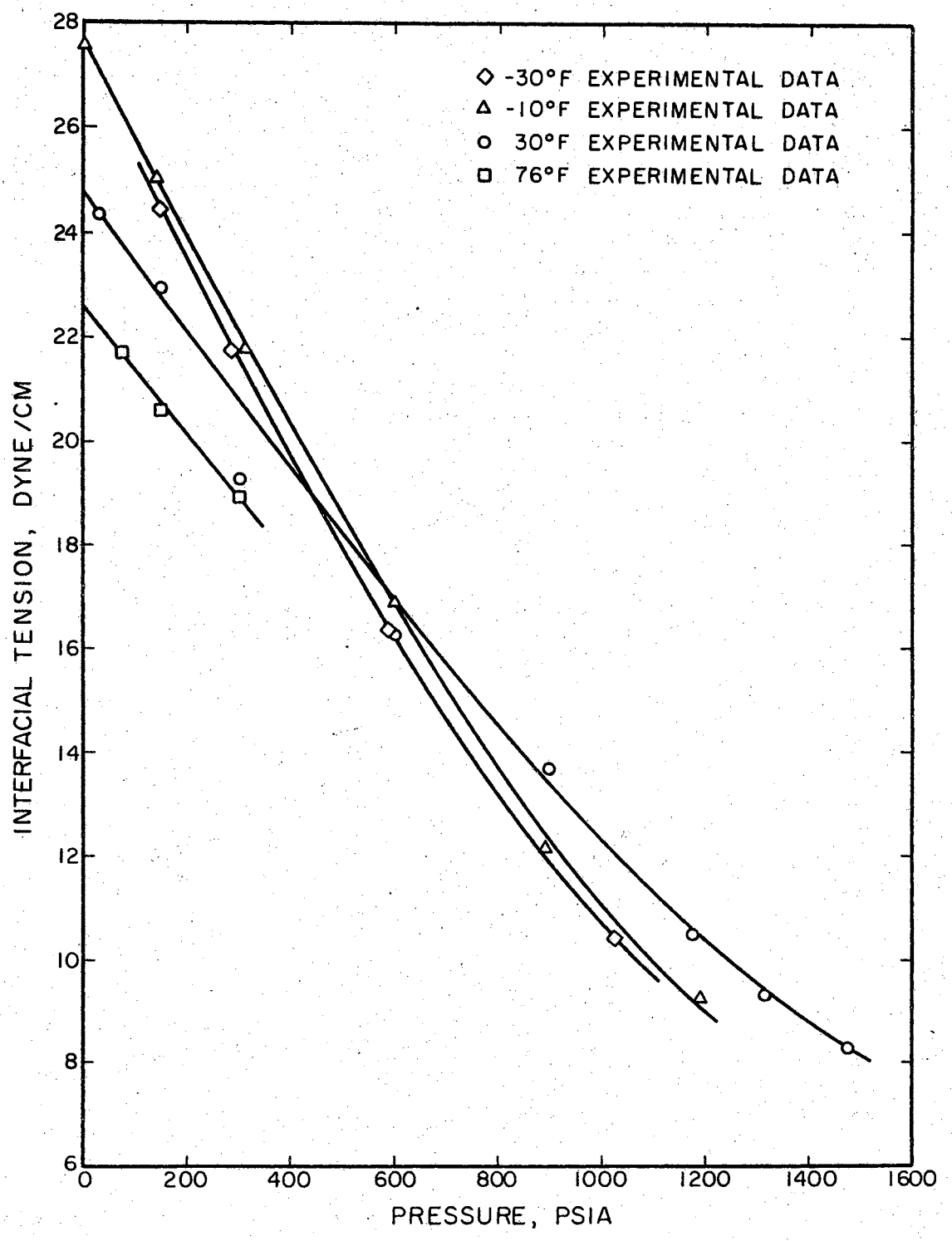

Figure 8. Isothermal Interfacial Tension of Methane-Nonane System

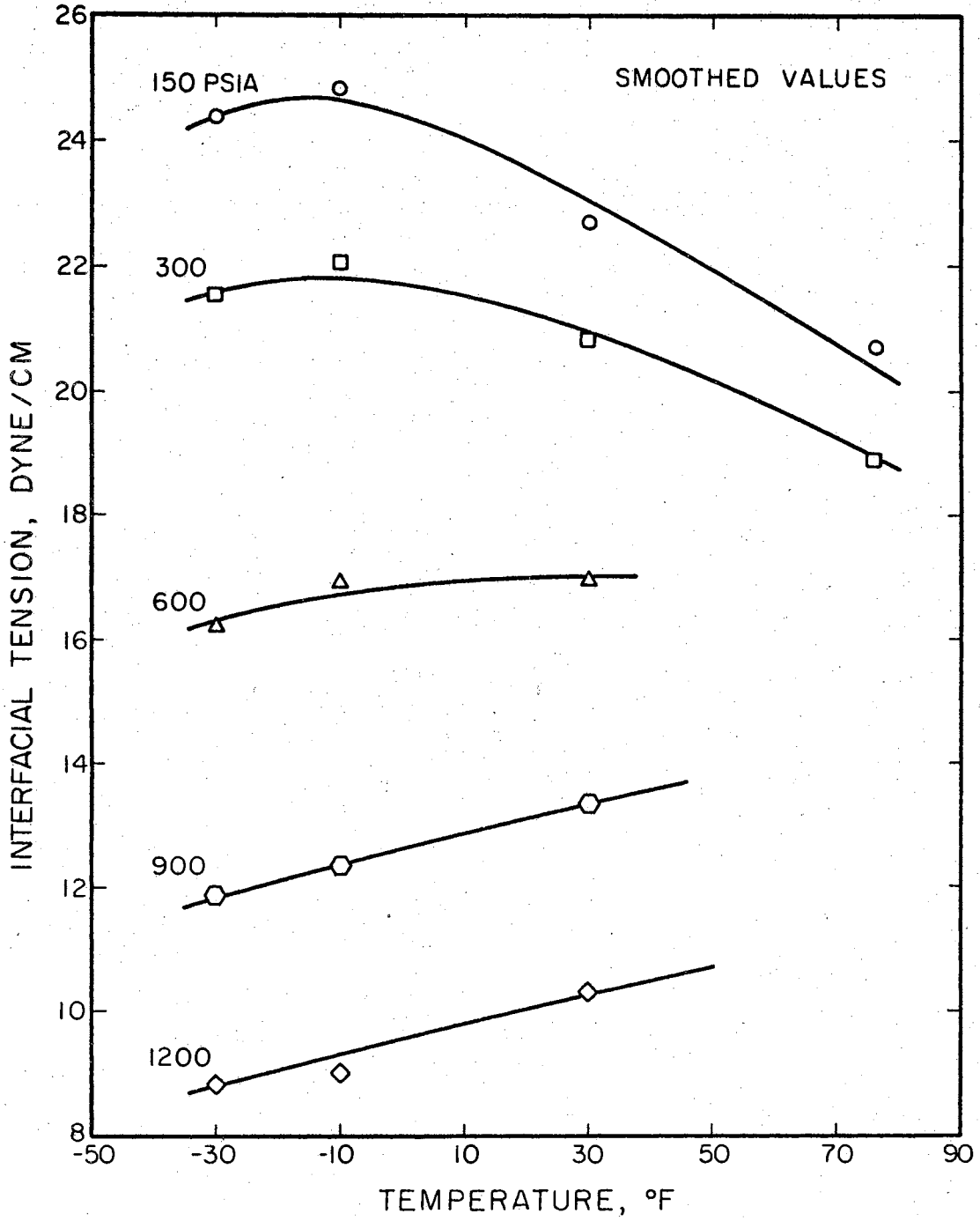

Figure 9. Interfacial Tension of Methane-Nonane System at Constant Pressure

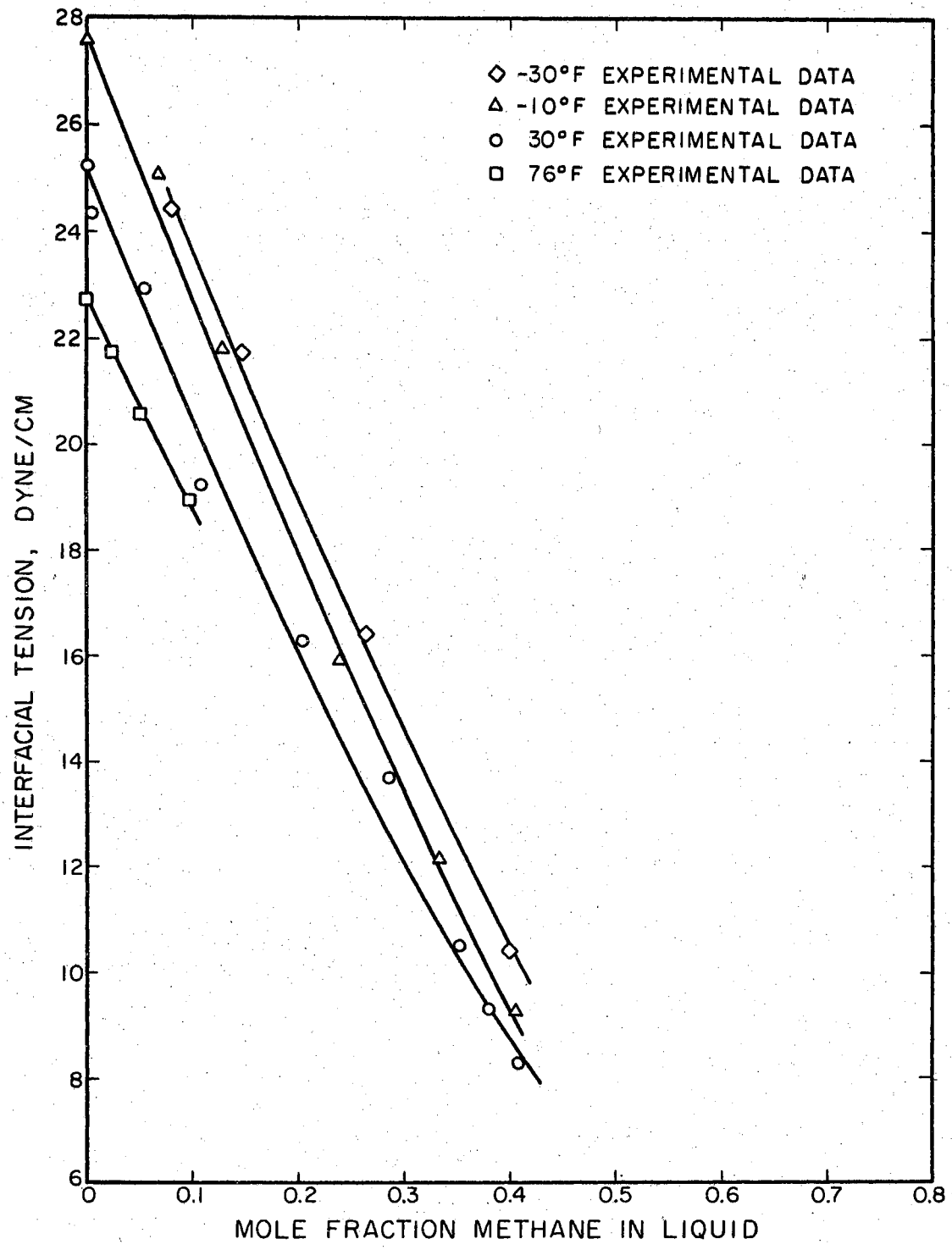

Figure 10. Interfacial Tension-Composition Diagram for Methane-Nonane System

TABLE IV

EXPERIMENTAL BUTANE-DECANE
INTERFACIAL TENSION

Composition Parameter	T °F	P psia	Exp. Value	Avg. Value
0.18	100	9	20.08 20.05 20.19 19.90	20.06
0.46	100	24	16.82 16.98 16.96	16.92
0.66	100	34	15.51 15.96	15.73
0.20	40	3.6	21.35 21.21 21.40	21.32

TABLE V

EXPERIMENTAL METHANE-BUTANE-DECANE INTERFACIAL TENSION

Composition Parameter	T °F	P psia	Exp. Value	Avg. Value	Composition Parameter	T °F	P psia	Exp. Value	Avg. Value
0.18	100	325	17.02 16.99 16.36	16.79	0.66	100	332	13.91 13.44 13.33 14.02	13.68
	100	685	13.85 14.05	13.95		100	671	11.81 11.57 11.78	11.72
	100	1145	10.95 10.79 11.00	10.91		100	1057	9.36 9.60 9.44 9.75	9.54
0.46	100	370	14.47 14.70 14.70 14.51 15.08	14.69	0.20	40	290	18.38 18.22 18.11	18.24
	100	730	12.87 12.61 12.71 12.79 12.42	12.68		40	555	14.66 14.45 14.71 14.58 14.87	14.65
	100	1120	9.95 9.79 10.05	9.93		40	1000	11.74 11.36 11.55	11.55

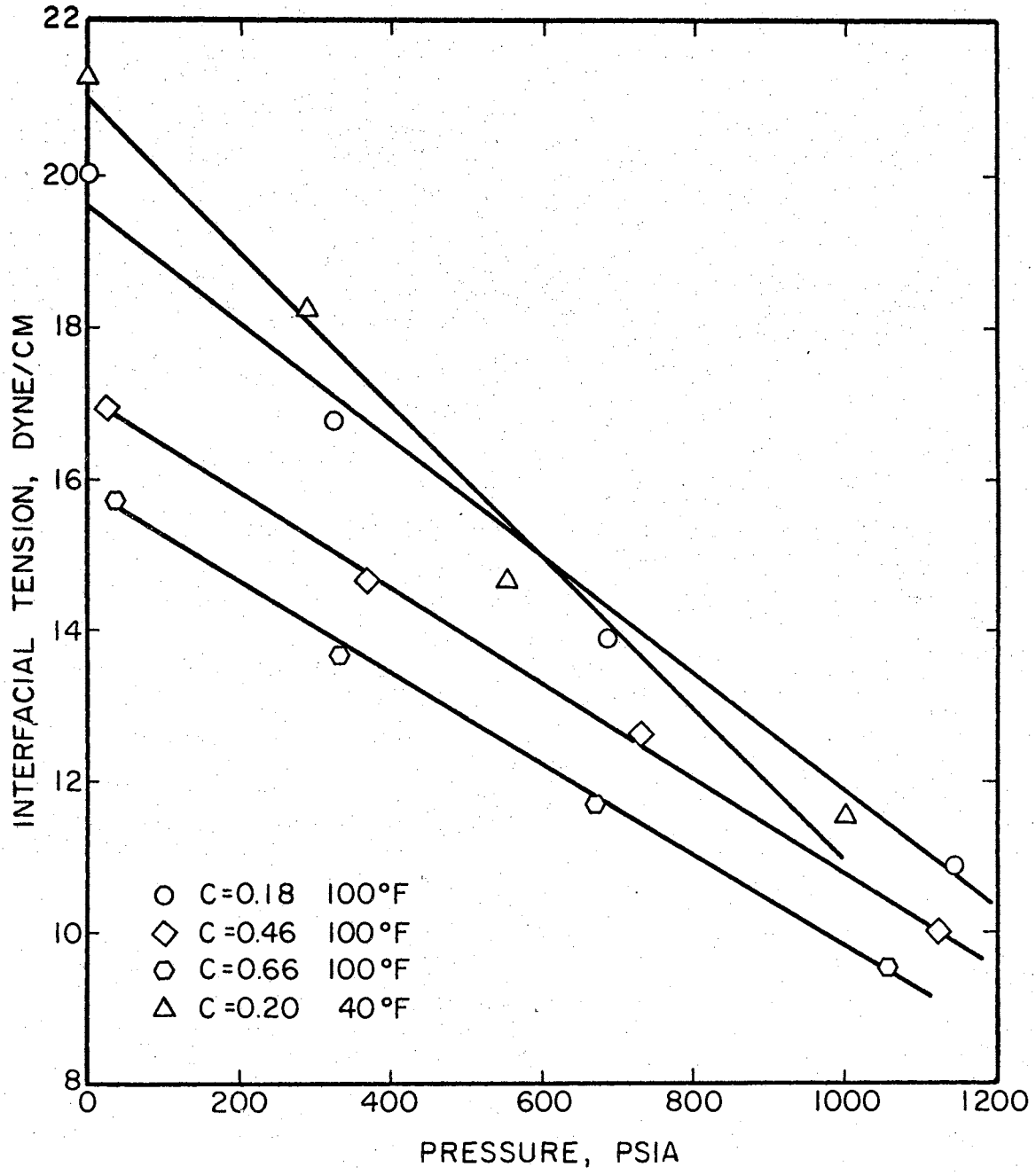

Figure 11. Interfacial Tension of Methane-Butane-Decane Mixtures at System Pressure

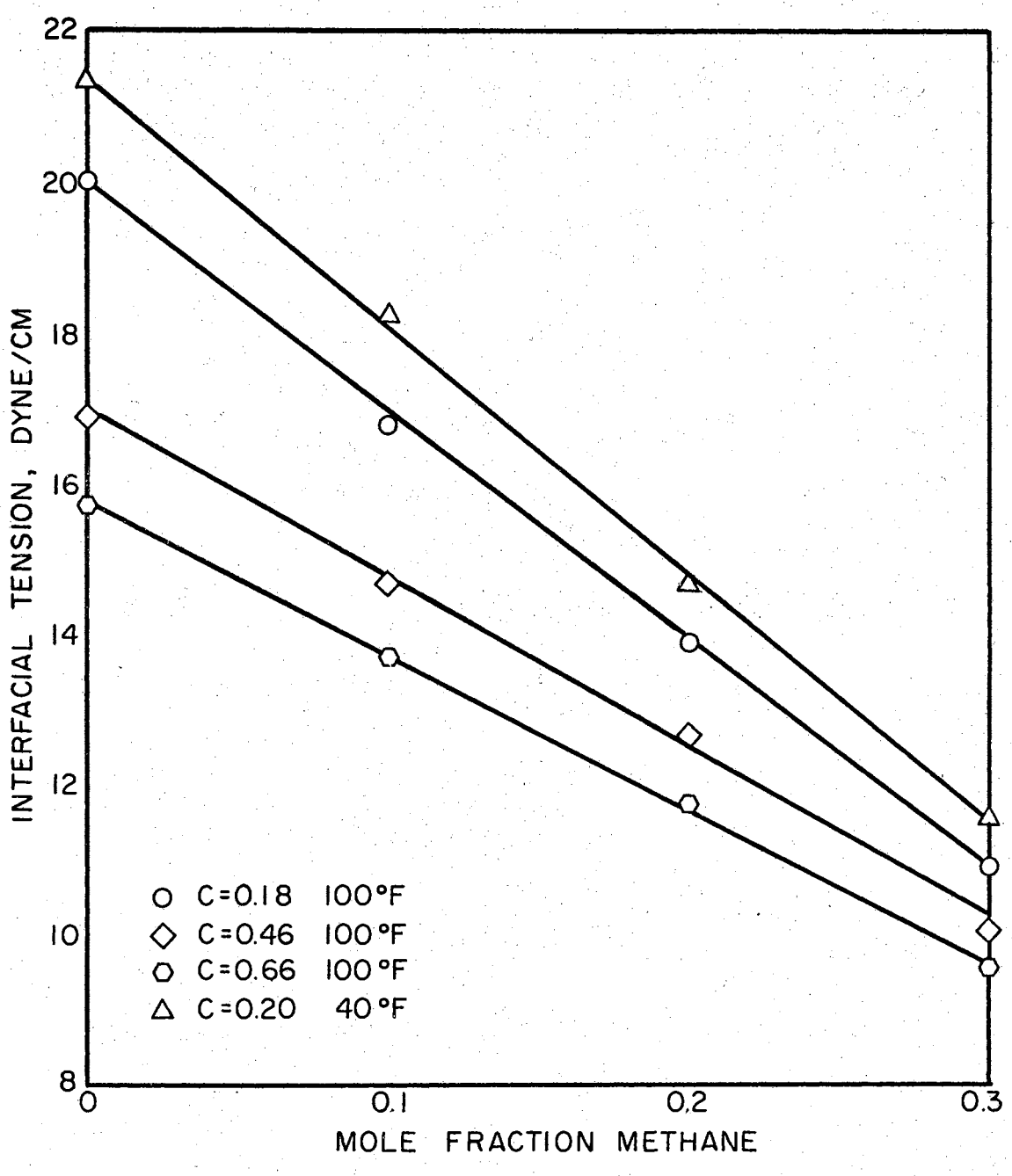

Figure 12. Interfacial Tension of Methane-Butane-Decane Mixtures as Function of Methane Concentration

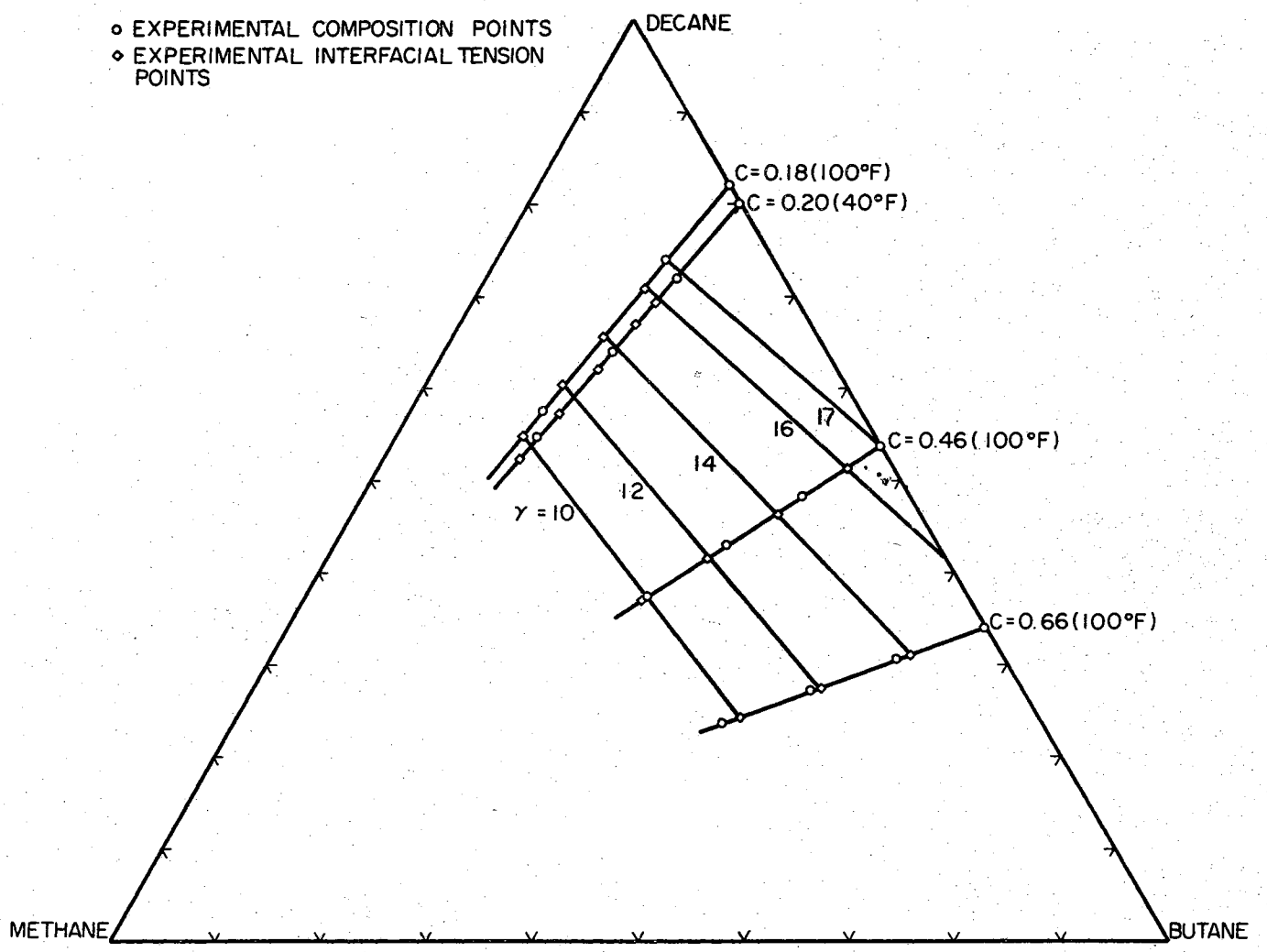

Figure 13. Phase Diagram for Methane-Butane-Decane Interfacial Tension

in equilibrium with the vapor phase. Interfacial tension values were calculated from drop measurements and phase densities by use of Equation (12).

CHAPTER VI

DISCUSSION OF RESULTS

Reliability of Experimental Data

The first experimental data were taken for comparison with literature work on pure nonane. Table VI shows a comparison of the experimental data taken from this work with the data of Jasper (21, 22). In general, the data show good agreement, with the average value in air being essentially the same as Jasper reports in a dry nitrogen atmosphere. The three experimental points show a total spread of four per cent based on the minimum value measured. The deviation from the average value is approximately ± 2 per cent. Also shown in Table VI are data for nonane in a methane atmosphere at one atmosphere pressure. These data show a slight effect on interfacial tension by the gaseous atmosphere, the values in methane being lower than those for corresponding temperature and pressure in air. The methane data show a total spread of 0.5 per cent based on the minimum value, with an average deviation of approximately ± 0.2 per cent.

Measurement errors account for at least part of the spread indicated by the experimental data in Table VI. A detailed examination of the errors involved in calculation

TABLE VI

RELIABILITY OF EXPERIMENTAL DATA

Surface Tension dynes/cm	Atmosphere	Source
22.48	nonane vapor	Jasper (21) (linear interpolation between 20°C and 30°C)
22.39	dry nitrogen	Jasper (22) (linear interpolation)
22.86 21.98 22.21	air	This work (77°F and 1 atm. dry air)
22.10 22.17 22.05	methane	This work (77°F and 1 atm.)

of experimental interfacial tension as a result of uncertainties in experimentally measured quantities is presented in Appendix A. An average value for the maximum diameter of a droplet in this work is approximately 0.25 cm. The Gaertner optical comparator is capable of measurements to 0.0001 cm. With the Gaertner comparator, the diameter of a droplet can be measured to a probable accuracy of 0.002 cm. The probable accuracy of diameter measurements is 0.001 cm. on the Vanguard motion analyzer which has a capacity for measurement to 0.001 inch on a projected magnified image. Because the equatorial diameter (d_e) and the selected plane diameter (d_s) enter into the interfacial tension calculations, both directly as shown in Equation (12), and indirectly through the relationship between 1/H and S, the effect of an error in measurement is multiplied by approximately five times in its effect on the interfacial tension. Thus, the limiting accuracy of the experimental measurements appears to be about ± 2 per cent of the average interfacial tension measurement. The experimental data shown in Table VI fairly well reflect the reproducibility and accuracy of the experimental apparatus and techniques used in this work.

Phase Rule Interpretation for Interfacial Tension

A discussion of the phase rule is useful in interpreting the behavior of interfacial tension, an intensive

variable, in the two-phase region for a two-component system. In accordance with the phase rule, for the state of equilibrium to be completely defined, two variables, e.g., temperature and pressure, must be fixed. Then the intensive properties of the coexisting phases are fixed. Fixing the temperature and pressure fixes the equilibrium composition of each phase and allows calculation of a unique interfacial tension value. This analysis permits determination of interfacial tension throughout the two-phase region and allows interpolation between data points, such as in Figures 8, 9, and 10.

Since undertaking a study for a ternary system is far more complex than for a binary system, a systematic procedure was selected for taking interfacial tension data for the ternary system. Otherwise, the relationship between the data would be extremely difficult to determine. The phase rule illustrates the problem; for a three-component system in the two-phase region, three variables must be fixed to define the state of equilibrium. Knowledge of the temperature and pressure alone is not sufficient to allow calculation of a unique value for the interfacial tension. Therefore, a composition parameter must be fixed. The method defined by Sage and workers (35) was used for the work reported here. Sage and workers used the concept of a constant-composition parameter expressed as

$$C = \frac{x_{C_4}}{x_{C_4} + x_{C_{10}}}. \qquad (26)$$

The use of a constant-composition parameter for the butane and decane components facilitates graphical operations associated with direct interpretation and interpolation of interfacial tension with respect to methane concentration and data smoothing. The runs on the methane-butane-decane system were based on constant-composition parameters of 0.18, 0.46, and 0.66 for the 100° F isotherm and a parameter of 0.20 for the 40° F isotherm.

Methane-Nonane Experimental Results

Liquid and vapor densities for experimental methane-nonane interfacial tension data were taken from the work of Shipman and Kohn (42). The only experimental density and composition data available in the literature on the methane-nonane system are those reported by Shipman and Kohn and Savvina (41). Savvina reports only liquid-phase compositions as a function of temperature and pressure, while Shipman and Kohn report phase compositions and phase volumes (or densities). Table VII compares the Savvina and the Shipman and Kohn liquid-phase compositions. In general, the data are in good agreement. Under the conditions of this work, the equilibrium constant for nonane never exceeds 0.01. For this reason, the gas phase may be assumed to be essentially pure methane for density calculations. Gas-phase densities calculated from methane

TABLE VII

COMPARISON OF KOHN AND SAVVINA EQUILIBRIUM DATA
METHANE-NONANE SYSTEM

T, °C	P atm	Methane mole fraction Shipman-Kohn (42)	Savvina (41)	Difference
100	10	.036	.030	.01
	20	.072	.075	--
	40	.139	.145	.01
	50	.172	.180	.01
	80	.263	.280	.02
	100	.319	.330	.01
150	10	.033	.025	.01
	20	.070	.070	--
	40	.114	.130	.02
	50	.173	.180	.01
	80	.261	.280	.02
	100	.312	.330	.02
50 (inter-polation)	10	.045	.045	--
	20	.086	.095	.01
	40	.162	.175	.01
	50	.197	.210	.01
	80	.291	.320	.03
	100	.347	.370	.02

Note: The Savvina values are limited in accuracy because they were read from a graph.

compressibility factors agree well with the vapor densities reported by Shipman and Kohn as shown in Table VIII.

The crossovers observed in Figure 8 are caused by the increase in concentration of methane relative to nonane in the mixture. Two counteracting effects are represented in the data. The interfacial tension value should be higher as colder temperatures are reached. But at the colder temperatures, the solubility of methane increases, tending to lower the interfacial tension.

Butane-Decane Experimental Results

Literature data on phase compositions and densities for the butane-decane binary and the methane-butane-decane ternary were not readily usable for interfacial tension calculations. Complete sets of phase compositions and densities were not available in the literature. Therefore, correlations were resorted to for specific cases for calculation of liquid and vapor density.

Liquid densities for the butane-decane points at 100° F were interpolated from the liquid density data of Reamer, Sage, and Lacey (34). The corresponding vapor densities were calculated from the Benedict-Webb-Rubin equation of state (5). Vapor densities calculated from butane compressibility factors were in good agreement with the BWR densities. The butane-decane liquid density at 40° F was calculated from the Rackett saturated-liquid density equation (31). The Rackett correlation was found to be

TABLE VIII

COMPARISON OF VAPOR DENSITIES FOR METHANE-NONANE SYSTEM

T, °F	P, psia	Gas-phase Density	
		Shipman (42)	NGPA Compressibility (27)
76	75	.00348	.00339
	150	.0067	.00682
	300	.0136	.0138
30	15	.00073	.00073
	150	.0076	.0075
	300	.0155	.0154
	600	.0325	.0325
	900	.0505	.0512
	1175	.0707	.0702
	1315	.0815	.0800
	1475	.0925	.0919
-10	140	.00814	.00772
	310	.0179	.0178
	598	.0368	.0371
	890	.0596	.0602
	1190	.0868	.0865
-30	147	.00854	.00856
	285	.0178	.0172
	590	.0393	.0391
	1025	.0828	.0801

the most accurate method for calculation of liquid density in this and other work. The Rackett method is presented in Appendix B. The corresponding bubble point pressure at 40° F was calculated from Raoult's law on the basis of the low value of the butane vapor pressure. The vapor density was calculated from the BWR equation.

Methane-Butane-Decane Experimental Results

For the 100° F ternary runs, phase data were taken from the work of Reamer, Sage, and Lacey (35, 36). However, only bubble point pressures were reported. Vapor compositions were calculated via the Chao-Seader (9) correlation using the computer program written by Erbar (11). Vapor densities were calculated via the BWR equation. Liquid and vapor compositions for the 40° F run were taken from the data of Sage and workers (40). The Rackett equation was used for the liquid density and the BWR equation for the vapor density.

Figures 11 and 12 show the effect of methane concentration and pressure on interfacial tension. As methane concentration increases with increasing system pressure, the interfacial tension of the mixture decreases. Figure 13 shows the range of composition over which the ternary data were taken. The phase diagram allows the mole fraction of each component to be plotted along with lines of constant interfacial tension. Figure 13 may be used to estimate the interfacial tension at 100° F for a mixture

when the composition falls in the outlined area. The data for the 40° F run with the composition parameter of 0.20 are superimposed on Figure 13 to show the relationship with the other data.

CHAPTER VII

CORRELATION OF INTERFACIAL TENSION DATA

Pure-component surface tension data can be accurately correlated by two methods described in the Literature Survey. These are the Ferguson (12) or van der Waals (48) equation

$$\gamma = \gamma_o (1 - T/T_c)^n \tag{27}$$

and the parachor relation of Sugden (47)

$$\gamma^{1/4} = \frac{[P]}{M} (d_L - d_V). \tag{28}$$

Interfacial tension data of binary mixtures have been correlated in the past mainly with the Weinaug-Katz (52) equation

$$\gamma^{1/4} = \frac{d_L}{M_L} \Sigma\, x_i [P_i] - \frac{d_V}{M_V} \Sigma\, y_i [P_i]. \tag{29}$$

This correlation was modified by Stegemeier and Hough (45) as

$$\gamma^{3/11} = \frac{d_L}{M_L} \Sigma\, x_i [P_i] - \frac{d_V}{M_V} \Sigma\, y_i [P_i]. \tag{30}$$

They based their modification on the density difference observations of Guggenheim (16) which give rise to a 3/11

exponent rather than the usually accepted 1/4 exponent. Stegemeier and Hough presented modified parachor values to use with Equation (30). Warren and Hough (50) further modified the parachor values to use with the 3/11 exponent from a regression analysis of interfacial tension data.

Recently Warren and Hough chose to use a modified form of the Sugden equation

$$\gamma = B(d_L - d_V)^E \qquad (31)$$

to correlate interfacial tension data. The values of B and E for seven binary systems varied from 41.33 to 122.58 for B and from 3.287 to 3.941 for E. Analysis of this new approach did not yield any firm conclusions.

The Weinaug-Katz relationship and the Stegemeier-Hough modification were used to correlate the experimental methane-nonane interfacial tension data taken in this study. Also, the Weinaug-Katz parachors were modified slightly to better reproduce the experimental data. Table IX shows a comparison of the experimental data with values calculated by the parachor relationships. The values calculated by the parachor relationships show good agreement, in general, with experimental data. However, the modified Weinaug-Katz relationship, in general, gives better reproducibility of experimental data for all temperature-pressure-composition ranges studied. Stegemeier values show a maximum of +19 per cent deviation with an average deviation of about +10 per cent. The Katz values agree

TABLE IX

COMPARISON OF PARACHOR CORRELATIONS WITH EXPERIMENTAL METHANE-NONANE DATA

T, °F	P, psia	Interfacial Tension				Per Cent Deviation		
		Avg. Exp.	Mod. Katz	Katz	Stegemeier	Mod. Katz	Katz	Stegemeier
-30	147	24.45	25.20	26.10	26.55	+3	+7	+8.7
	285	21.73	22.71	23.54	24.18	+4.5	+8.3	+11.2
	590	16.38	17.75	18.45	19.42	+8	+12	+18.5
	1025	10.41	10.50	11.04	12.33	+1	+6	+18.5
-10	140	25.05	24.43	25.32	25.84	-2.5	+1	+3
	310	21.79	21.82	22.64	23.37	+0.1	+4	+7
	598	15.91	17.53	18.23	19.22	+10	+14	+18
	890	12.16	13.32	13.92	15.11	+9.5	+14	+19
	1190	9.27	9.43	9.94	11.23	+1.7	+7	+18
30	15 (air)	25.25						
	15	24.37	24.19	25.05	24.80	-.74	+3	+1.7
	150	22.95	22.43	23.27	23.19	-2.3	+1	+1
	300	19.27	20.45	21.24	21.36	+6.1	+10	+11
	600	16.28	16.67	17.37	17.84	+2.4	+7	+9.6
	900	13.68	13.43	14.05	14.75	-1.8	+3	+7.8
	1175	10.48	10.38	10.94	11.81	-1	+4	+12.6
	1315	9.30	9.01	9.49	10.46	-3.1	+2	+12.5
	1475	8.26	7.84	8.29	9.29	-5.1	0	+12.5
76	15 (air)	22.76						
	75	21.77	20.59	21.34	21.41	-5.4	-2	-1.7
	150	20.58	19.86	20.58	20.73	-3.5	0	+0.7
	300	18.93	18.36	19.06	19.34	-3	+1	+2.2

within a maximum deviation of +14 per cent and an average absolute deviation of approximately 5 per cent. The modified parachor values for the Weinaug-Katz relationship give a maximum deviation of +10 per cent and an average absolute deviation of approximately 4 per cent. The parachor values used in each procedure are shown in Table X.

The methane-butane-decane experimental results were correlated with the Weinaug-Katz and Stegemeier-Hough expressions, extended to include three components. The results of the comparison are presented in Table XI. In general, both correlations give about the same error. For the Weinaug-Katz correlation, the maximum positive and negative deviations are 12.6 and 24.3 per cent, respectively, while the average absolute error is 7.8 per cent. The Stegemeier-Hough values show a maximum positive deviation of 14.3 per cent, maximum negative deviation of 18.9 per cent, and average absolute deviation of 7.0 per cent. The parachor values used for these correlations are included in Table X.

In an effort to obtain better agreement between experimental and calculated interfacial tension, the effect of various hydrocarbon solvents on the value of the methane parachor was examined. The best parachor value for methane was determined from regression analysis of binary and ternary interfacial tension data using the Weinaug-Katz relationship. The parachor value used for

TABLE X

COMPARISON OF PARACHOR VALUES

	Methane	Nonane	Butane	Decane
Weinaug-Katz	77.9	391.0	189.9	431.0
Stegemeier-Hough	77.9	423.0	200.5	463.0
Modified Weinaug-Katz	81.0	387.6		

TABLE XI

COMPARISON OF PARACHOR CORRELATIONS WITH EXPERIMENTAL BUTANE-DECANE AND METHANE-BUTANE-DECANE DATA

Composition Parameter	T, °F	P, Psia	Interfacial Tension			Per Cent Error	
			Avg. Exp.	Katz	Stegemeier	Katz	Stegemeier
0.18	100	9	20.06	21.13	21.18	+5.3	+5.6
	100	325	16.79	17.39	17.78	+3.6	+5.9
	100	685	13.95	13.83	14.47	-0.9	+3.7
	100	1145	10.91	11.36	10.98	+4.1	+0.6
0.46	100	24	16.92	18.59	18.47	+9.9	+9.1
	100	370	14.69	15.40	15.62	+4.7	+6.3
	100	730	12.68	12.11	12.57	-4.5	-0.9
	100	1120	9.93	8.80	9.41	-11.4	-5.2
0.66	100	34	15.73	16.08	16.00	+2.2	+2.0
	100	332	13.68	13.26	13.45	-3.0	-1.1
	100	671	11.72	10.07	10.66	-14.0	-9.0
	100	1057	9.54	7.23	7.74	-24.3	-18.9
0.20	40	3.6	21.32	24.02	23.80	+12.6	+11.6
	40	290	18.24	20.35	20.50	+11.5	+12.4
	40	555	14.65	16.56	17.01	+11.5	+14.3
	40	1000	11.55	11.33	12.13	-2.2	+5.0

the solvent component was the pure-component parachor value for that substance. Table XII shows the pure-component solvent parachor and the best methane parachor calculated from interfacial tension data for each system. Also, the error involved in predicting interfacial tension using the best methane parachor is given.

Table XII shows that the calculated value of the methane parachor in a mixture is not constant, but increases with carbon number to pentane and then decreases. No reason was found for the maximum value to occur at pentane. Reno and Katz (38) found a similar behavior with nitrogen in butane and in heptane. They calculated a parachor value for nitrogen of 60 in the butane solvent and 41 in the heptane solvent. The value for the parachor for nitrogen from pure-component surface tension data of nitrogen is 60.

A possible explanation for the variation in the methane parachor in different solvents is that methane above its critical temperature behaves as a dissolved gas instead of a condensable vapor. At experimental conditions for the systems in Table XII, methane is above its critical temperature. Figures 14 and 15 relate the variation in methane parachor to characteristic properties of the solvent. Figure 14 is a plot of the best methane parachor and acentric factor of the solvent. Figure 15 shows a similar effect with solubility parameter of the solvent.

TABLE XII

BEST VALUE OF METHANE PARACHOR IN HYDROCARBON SOLVENTS

System	Solvent Parachor	Best Methane Parachor	Per Cent Error in Interfacial Tension		
			Maximum Positive	Maximum Negative	Average Absolute
Methane-Propane	150.3	90	12.78	10.14	2.42
Methane-Butane	189.9	130	38.73	12.09	5.52
Methane-Pentane	231.5	290	1.59	38.01	13.74
Methane-Heptane	312.0	155	9.34	2.68	3.53
Methane-Nonane	391.0	90	12.96	6.41	4.39
Methane-Decane	431.0	40	11.07	7.23	3.35
Methane-Butane-Decane	189.9 431.0	67	14.34	23.75	7.63

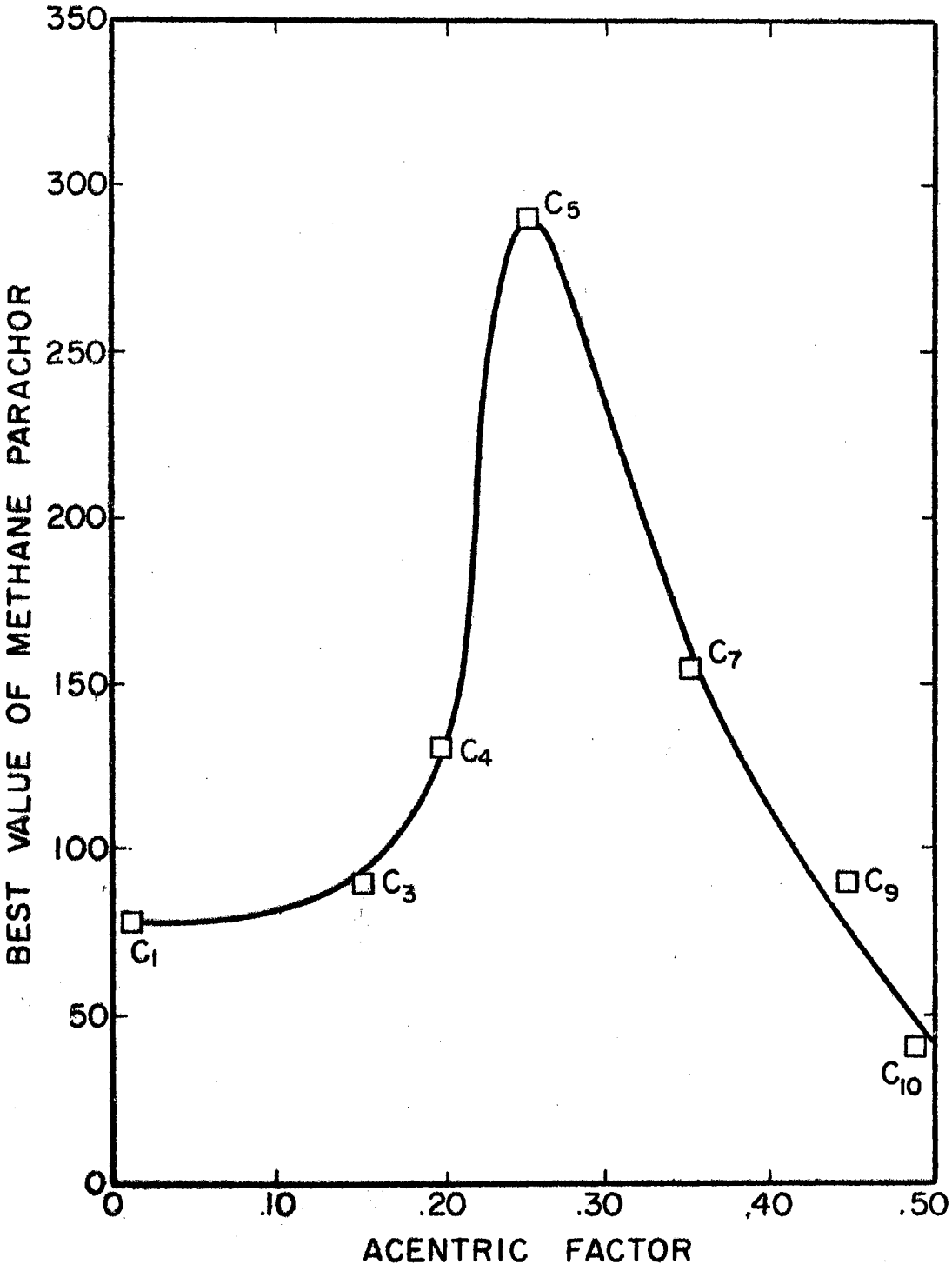

Figure 14. Best Value of Methane Parachor Versus Solvent Acentric Factor

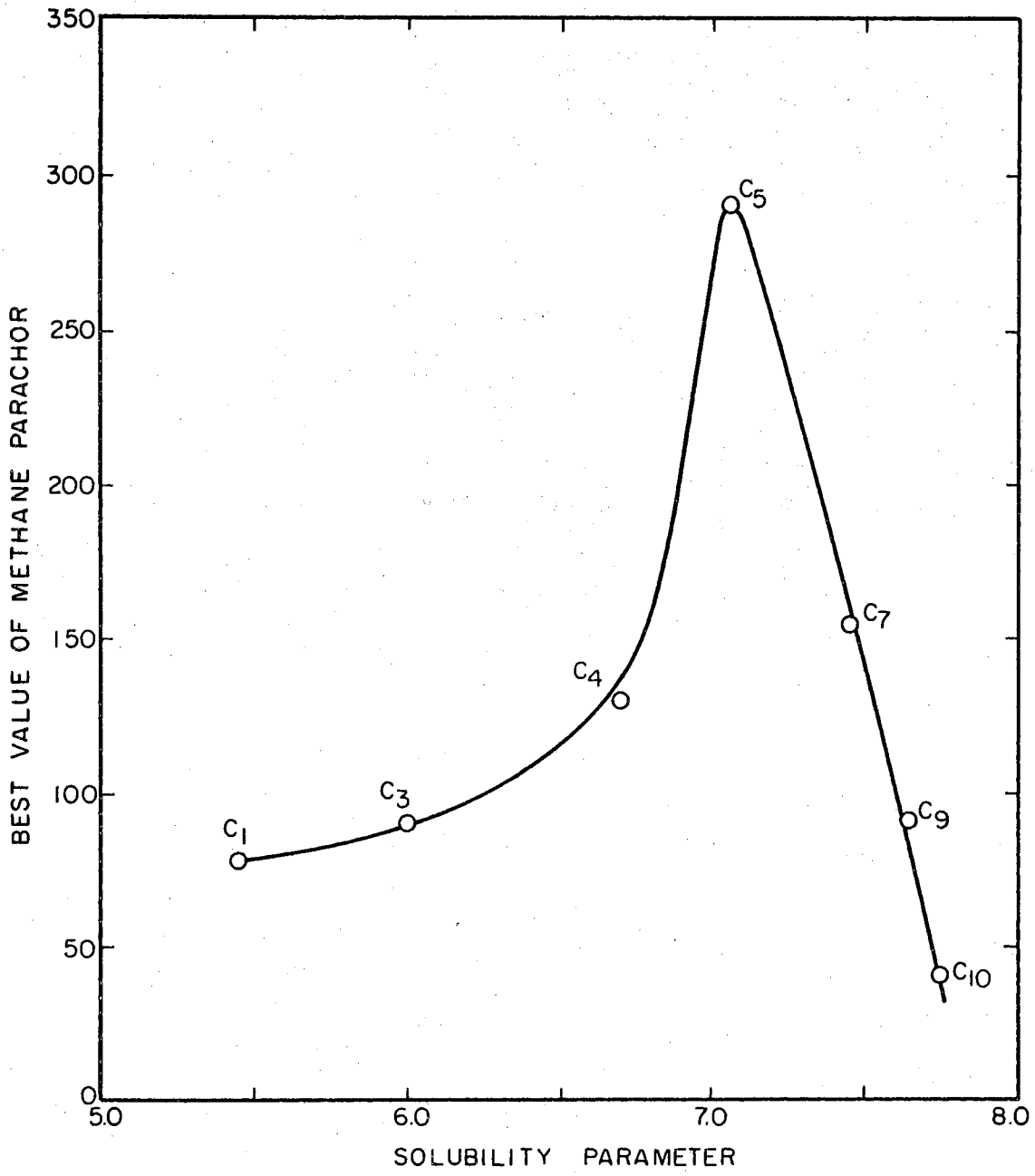

Figure 15. Best Value of Methane Parachor Versus Solvent Solubility Parameter

The best-methane-parachor concept was applied to methane-butane-decane data to test its extension to multicomponent systems. Table XII shows that the best parachor value for methane in butane and decane is 67. Parachor values in Table XII have been made temperature- and composition-independent by calculating the best methane parachor from a regression analysis of data over a temperature and composition range. Therefore, for a solvent mixture of butane and decane, the mixture acentric factor or solubility parameter should be a composition-independent quantity. Using arithmetic-average acentric factor and solubility parameter for the butane-decane solvent, the methane parachor values taken from Figures 14 and 15 are 160 and 250, respectively. These values deviate significantly from the best-fit value of 67, indicating that the best methane parachor cannot be accurately predicted from Figures 14 and 15 for multicomponent systems.

In relation to the dissolved-gas behavior of methane, an approach for correlating interfacial tension at moderate pressures from pure-component surface tension data was examined. The equation proposed for this analysis was

$$\gamma_m = x_2\gamma_2 - x_1\omega_2 T_{r_1}\gamma_1 . \qquad (32)$$

Equation (32) takes into account two effects. The character of the solvent enters through the acentric factor ω_2. Also, the fact that methane effectively lowers the interfacial tension of the liquid by acting as a dissolved gas

above its critical temperature is indicated by T_{r_1}, which is the system temperature divided by the methane critical temperature. T_{r_1} is always greater than unity for the mixtures investigated in this study. The pure-component surface tension for each component was calculated using the Ferguson equation at the pseudo-reduced temperature of the mixture. Constants for the Ferguson equation are given in Appendix C. The pseudo-critical temperature for the mixture was calculated by the technique proposed by Rackett (31) for mixture liquid density. The Rackett method is illustrated in Appendix B. Table XIII shows the results obtained with Equation (32). Equation (32) was modified for the methane-butane-decane system by adding the $x_3\gamma_3$ term to the right-hand side. In general, the results are slightly better than results obtained by the parachor techniques. The methane-butane and methane-decane systems show poor agreement. Lack of agreement for these systems may be due to low interfacial tension values at high pressures (1300-5000 psia).

In further examination of the dissolved-gas effect of methane, the most successful method found for a wide temperature-pressure-composition range was a correlation in the form of excess interfacial tension defined by

$$\gamma^E = \gamma_m - \Sigma\, x_i \gamma_i \qquad (33)$$

γ^E is the excess interfacial tension, γ_m is the experimental mixture interfacial tension, and γ_i is the

TABLE XIII

INTERFACIAL TENSION FROM PURE-COMPONENT SURFACE TENSION

System	Temperature Range, °F	Pressure Range, psia	Per Cent Deviation		
			Max. Pos.	Max. Neg.	Avg. Absolute
Methane-Propane	86-149	220-830	18.2	-	6.3
Methane-Butane	100-160	1300-1500	181.9	-	104.3
Methane-Pentane	100-160	600-1500	8.7	-	5.2
Methane-Heptane	100	200-1000	2.6	0.8	1.0
Methane-Nonane	-30-76	15-1500	8.6	5.3	3.3
Methane-Decane	100-160	1500-5000	-	225.5	89.9
Methane-Butane-Decane	40-100	325-1145	13.3	2.5	6.0

pure-component surface tension. Pure-component surface tension values were calculated from the Ferguson equation and the pseudo-reduced temperature procedure described above. The range of excess interfacial tension values is listed in Table XIV. Excess interfacial tension values for each data point are presented in Appendix C. Table XIV shows that the excess interfacial tension values for each system are negative, indicating a dissolved methane effect of lowering the interfacial tension of the mixture.

Figure 16 shows a plot of excess interfacial tension against mole fraction methane in the liquid for isotherms for the methane-pentane and methane-decane systems. The data show a decrease (increasingly negative) in excess interfacial tension to a minimum value and then an increase with increasing methane concentration. The data also show that interfacial tension can be correlated with an excess function, since the isothermal curves indicate that the excess values go to zero at the pure-component end points.

Excess interfacial tension values were related to methane concentration and pseudo-reduced temperature by Figure 17. The excess values were plotted against methane concentration. Lines of constant reduced temperature were drawn through data points having the same, or nearly the same, pseudo-reduced temperature. With Figure 17 thus constructed, the excess interfacial tension for each data point was determined from the plot and compared with the value calculated from Equation (33). Table XV shows the

TABLE XIV

EXCESS INTERFACIAL TENSION VALUES

System	Temperature Range, °F	Pressure Range, psia	Range of Excess Interfacial Tension
Methane-Propane	86 - 149	220 - 1300	-1.168 - 0.004
Methane-Butane	100 - 160	1300 - 1500	-3.745 - -1.950
Methane-Pentane	100 - 160	600 - 2250	-4.257 - -1.597
Methane-Heptane	100	200 - 1000	-5.300 - -1.475
Methane-Nonane	-30 - 76	15 - 1500	-12.486 - -0.105
Methane-Decane	100 - 160	1500 - 5000	-12.304 - -6.335
Methane-Butane-Decane	40 - 100	325 - 1145	-9.568 - -3.071

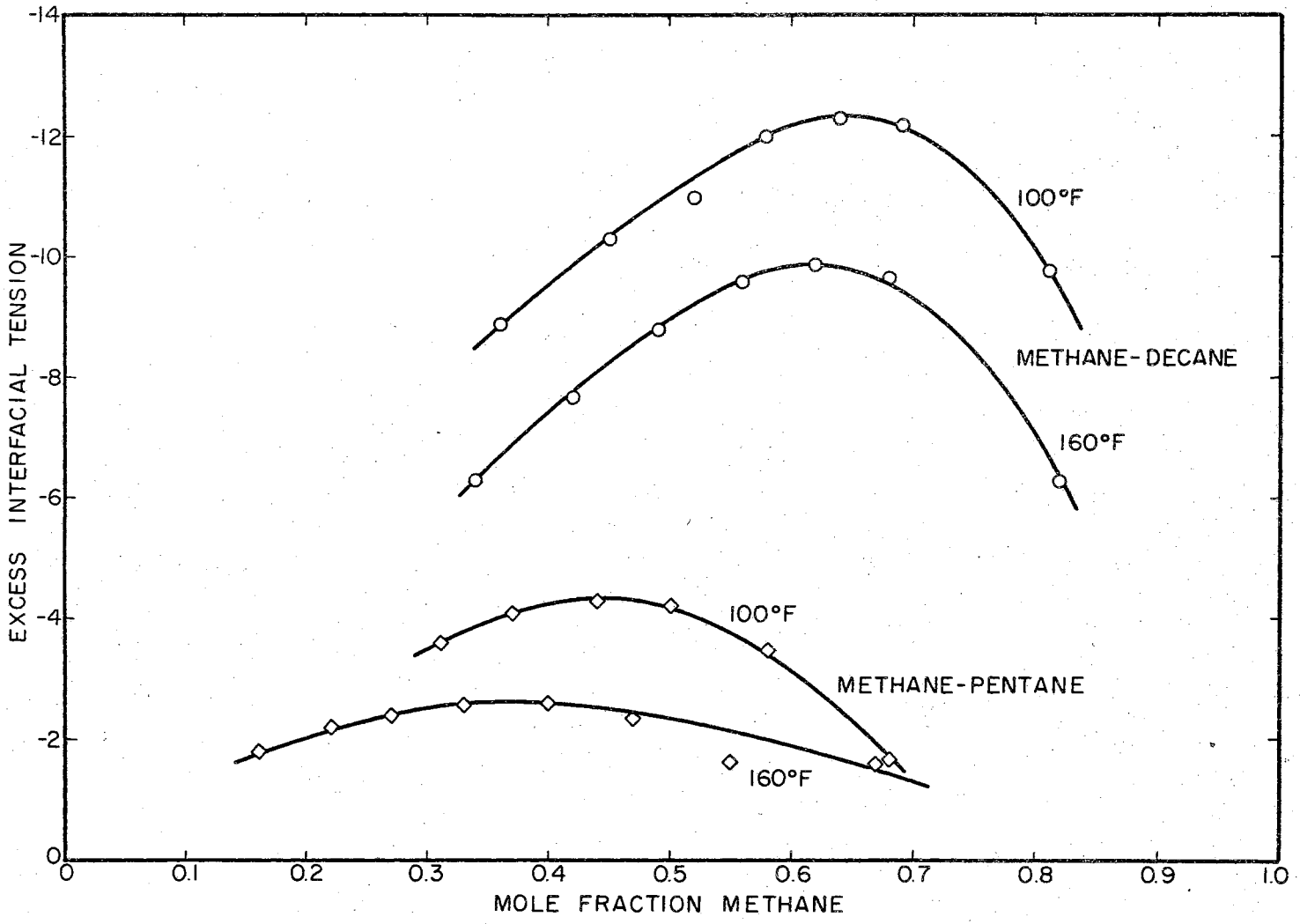

Figure 16. Isothermal Excess Interfacial Tension

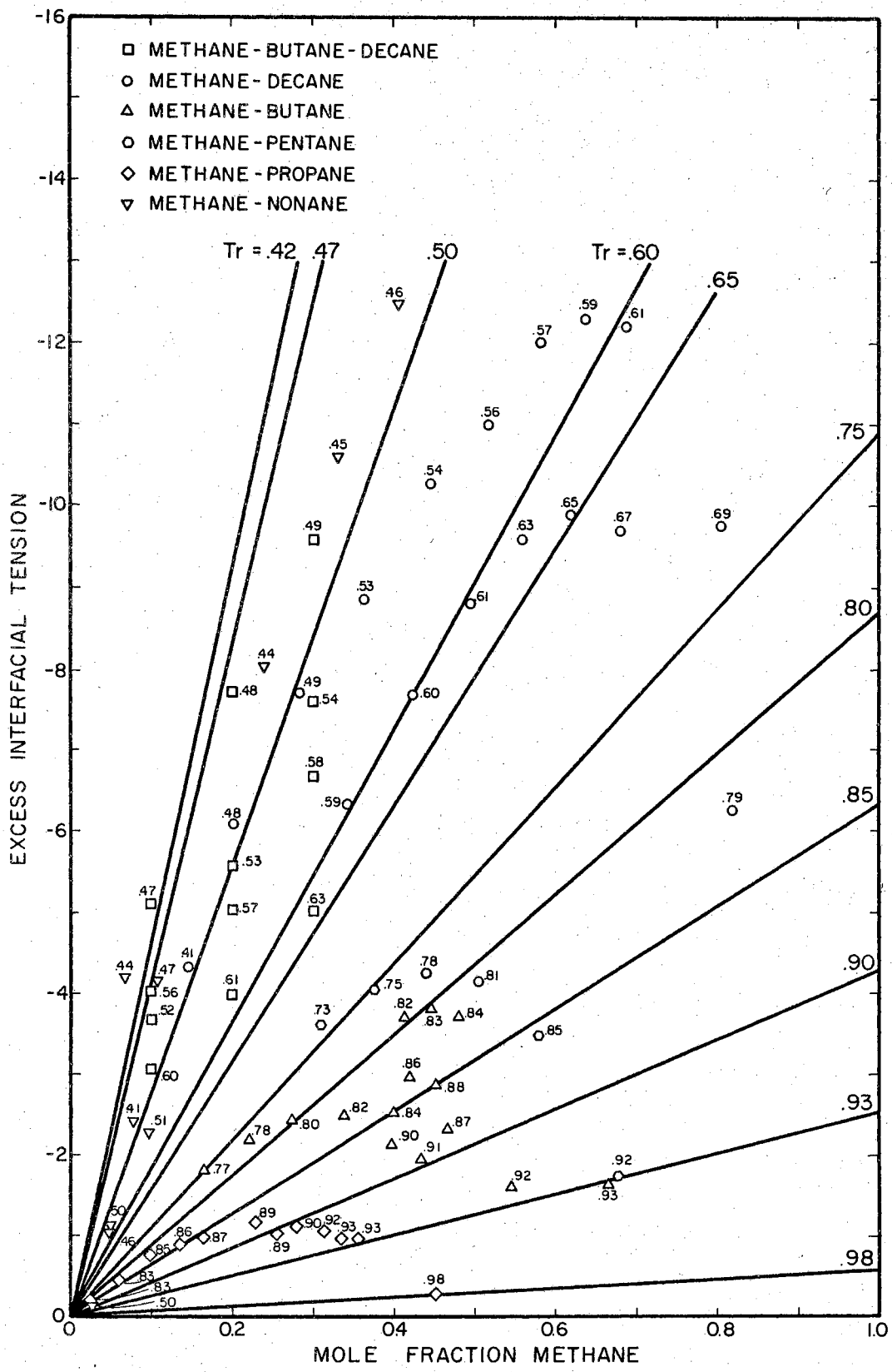

Figure 17. Excess Interfacial Tension as Function of Methane Concentration and Reduced Temperature

TABLE XV

ANALYSIS OF EXCESS INTERFACIAL TENSION CORRELATION

System	T, °F	P, psia	Per Cent Error in Calculated Interfacial Tension
Methane-Propane	86	583	-0.3
		808	-7.0
		948	-2.6
		1039	+7.0
		1230	-1.5
Methane-Butane	100	1300	+17.5
		1400	+27.4
		1500	+40.0
	130	1400	+30.2
		1500	+62.8
	160	1400	+39.4
		1500	+67.8
Methane-Pentane	100	1000	-0.6
		1250	-1.0
		1500	-0.7
		1750	-3.3
		2000	-20.2
	160	600	+2.0
		800	+1.6
		1000	+0.8
		1250	-5.0
		1500	-4.9
		1750	-8.8
Methane-Heptane	100	200	+1.0
		400	+1.5
		600	+2.0
		800	+6.4
		1000	+3.8
Methane-Nonane	76	75	-2.2
		150	-1.0
		300	-2.1
	30	150	-6.0
		600	-15.2
		900	-13.6
		1175	+1.5
		1475	+0.8
	-10	140	-8.7
		598	-12.6
		890	-23.6

TABLE XV (Continued)

System	T, °F	P, psia	Per Cent Error in Calculated Interfacial Tension
Methane-Decane	100	1500	-2.3
		2000	-4.2
		2500	-7.8
		3000	+4.1
		3500	+12.4
		4000	-0.6
	160	1500	-0.1
		2000	+0.2
		2500	+1.5
		3000	+4.9
		3500	+0.8
		4000	-26.0
Methane-Butane-Decane	100	325	+6.7
		685	+4.4
		1145	+4.0
		370	+8.6
		730	+6.1
		1120	+6.8
		332	+8.9
		671	+1.9
		1057	+6.8
	40	290	+2.1
		555	-4.7
		1000	+0.3

error in calculated interfacial tension by using Figure 17 as a predictive method for methane in various paraffin hydrocarbon solvents.

Interfacial tension data for the nitrogen-heptane and ethylene-heptane systems were used to test the applicability of Figure 17 to non-methane light components. At experimental conditions for these systems, nitrogen and ethylene are above their critical temperatures and should behave, similar to methane, as dissolved gases. Table XVI shows the comparison between experimental interfacial tension and interfacial tension calculated by use of Equation (33) and Figure 17 for the nitrogen-heptane and ethylene-heptane systems. The deviations are reasonable considering the fact that only data for methane in heavier hydrocarbons were used in constructing Figure 17. Indications are that Figure 17 can be used not only for methane in hydrocarbon mixtures, but also for other light components, such as nitrogen and ethylene, in heavier hydrocarbons.

TABLE XVI

EXCESS INTERFACIAL TENSION FOR NITROGEN-HEPTANE AND ETHYLENE-HEPTANE SYSTEMS

System	T, °F	P, psia	Per Cent Error in Interfacial Tension
Nitrogen-Heptane	77	214	+1.0
	77	514	+3.7
	77	1014	+9.9
	131	214	+1.0
	131	514	+6.5
	131	1016	+13.0
	185	214	+3.0
	185	513	+7.3
	185	1001	+9.7
Ethylene-Heptane	100	200	-10.6
	100	400	-23.1
	100	600	-38.2
	160	200	-4.7
	160	400	-12.4
	160	600	-19.3

CHAPTER VIII

CONCLUSIONS AND RECOMMENDATIONS

Conclusions

The objectives of this investigation were to measure and correlate the interfacial tension of saturated liquid mixtures of methane and heavier hydrocarbons in equilibrium with the corresponding vapor phase. Experimental data were obtained by using a high-pressure pendant drop apparatus. Experimental interfacial tension data were obtained for the methane-nonane and butane-decane binary systems and the methane-butane-decane ternary system. These data were used to show the effect of methane concentration on the interfacial tension of hydrocarbon systems.

Experimental data from this study and literature data were used to test the applicability of existing correlations in the literature. In general, the literature parachor methods were only moderately successful in correlating interfacial tension data.

The Weinaug-Katz parachor correlation was modified to better fit experimental data from several binary systems and the methane-butane-decane system. The methane parachor was found to have a different value in each hydrocarbon system investigated. The variation in the methane parachor

value was attributed to the fact that methane above its critical temperature behaves as a dissolved gas, instead of a condensable vapor, in the hydrocarbon solvent. The maximum value found for the methane parachor occurred for methane dissolved in pentane. No reason was found for the maximum value to occur at pentane.

Interfacial tension data at pressures up to about 1500 psia for several methane-heavier hydrocarbon systems were correlated accurately with an equation relating the character of the solvent component and the dissolved-gas effect of methane. Large deviations were found at higher pressures for systems having low interfacial tension values.

On the basis of the dissolved-gas behavior of methane, a method in the form of excess interfacial tension was developed to correlate interfacial tension data over a wide temperature-pressure-composition range. Excess interfacial tension values for several systems of methane in a heavier hydrocarbon were related to methane concentration and pseudo-reduced temperature. Interfacial tension data from atmospheric pressure to about 4000 psia were accurately correlated by this method.

Analysis of nitrogen-heptane and ethylene-heptane interfacial tension data showed that the excess interfacial tension concept could also be used for light components other than methane.

Recommendations

For future studies of interfacial tension, a reliable method for obtaining experimental liquid density should be added to the experimental apparatus. This is particularly important when dealing with systems and experimental conditions for which no experimental density data are available in the literature. Also the density equipment should provide a check on experimental literature density data which have doubtful accuracy. Finally, many of the liquid mixtures in gas processing and other operations contain a substantial amount of dissolved gases such as carbon dioxide and hydrogen sulfide. Future experimental work should be concerned with determination of interfacial tension for mixtures containing these dissolved gases. Experimental data on these systems should provide a test of the generality of the excess interfacial tension concept.

NOMENCLATURE

Major Symbols

English Letters

b	radius of curvature of drop at origin
	weighting factor for Rackett density equation
C	constant composition parameter
d	density
d_e	equatorial diameter
d_s	selected plane diameter
g	acceleration of gravity
H	shape dependent parameter
k	constant in Eotvos equation
M	molecular weight
n	exponent in van der Waals and Ferguson equations
P	pressure difference across a curved interface
	pressure
[P]	parachor
R and R′	principal radii of curvature for curved surface
s	arc length on drop profile
S	experimentally measurable drop shape factor
T	absolute temperature

V	volume
x	drop co-ordinate
	mole fraction in liquid phase
y	mole fraction in vapor phase
z	vertical co-ordinate measured from bottom of drop
	compressibility factor

Greek Letters

α_c	Riedel critical parameter
β	drop shape factor
δ	degrees in absolute temperature
γ	surface or interfacial tension
γ_o	van der Waals or Ferguson constant
γ^E	excess interfacial tension
ω	acentric factor
φ	angle for drop profile
ρ	radius of curvature
$\Delta\rho$	density difference between liquid and vapor phases

Subscripts

c	critical property
i	component number
L	liquid phase
m	mixture value
r	reduced property

s	saturated or equilibrium property
V	vapor phase

A SELECTED BIBLIOGRAPHY

1. Adamson, A. W. Physical Chemistry of Surfaces. New York: Interscience Publishers, Inc., 1960.

2. Andreas, J. M., E. A. Hauser, and W. B. Tucker. Journal of Physical Chemistry 42, 1001 (1938).

3. American Petroleum Institute (API) Technical Data Book --- Petroleum Refining (1966).

4. Bashforth, F., and J. C. Adams. "An Attempt to Test the Theories of Capillary Action." University Press, Cambridge, England (1883).

5. Benedict, M., G. B. Webb, and L. C. Rubin. Chemical Engineering Progress 47, 419 (1951).

6. Bowden, S. T., and E. T. Butler. Journal of Chemical Society, 754 (1939).

7. Brauer, E. B., and E. W. Hough. Producers Monthly 29 (8), 13 (1965).

8. Brock, J. R., and R. B. Bird. A. I. Ch. E. Journal 1, 174 (1955).

9. Chao, K. C., and J. D. Seader. A. I. Ch. E. Journal 7, 598 (1961).

10. Eotvos, R. Annalen der Physik und Chemie N. F. 27, 448 (1886).

11. Erbar, J. H., C. L. Persyn, and W. C. Edmister. "Enthalpies and K-Ratios for Hydrocarbon Mixtures by New Improved Computer Program." NGPA Proceedings, p. 26 (1964).

12. Ferguson, A. Transactions of Faraday Society 19, 407 (1923).

13. Fordham, S. Proceedings of Royal Society (London) 194A, 1 (1948).

14. Fowler, R. H. Proceedings of Royal Society (London) 159, 229 (1937).

15. Gambill, W. R. Chemical Engineering 65 (7), 146 (1958); 65 (9), 143 (1958).

16. Guggenheim, E. A. Journal of Chemical Physics 13, 256 (1945).

17. Hammick, D. L., and L. W. Andrew. Journal of Chemical Society, 754 (1929).

18. Harmens, A. Chemical Engineering Science 20, 813 (1965).

19. Hirschfelder, J. O., C. F. Curtiss, and R. B. Bird. Molecular Theory of Gases and Liquids. New York: John Wiley and Sons, 1954.

20. Hough, E. W., B. B. Wood, and M. J. Rzasa. Journal of Physical Chemistry 56, 996 (1952).

21. Jasper, J. J., E. R. Kerr, and F. Gregorich. Journal of American Chemical Society 75, 5252 (1953).

22. Jasper, J. J., and E. V. Kring. Journal of Physical Chemistry 59, 1019 (1955).

23. Lowry, T. M. Nature 125, 364 (1930).

24. Maass, O., and C. H. Wright. Journal of American Chemical Society 43, 1098 (1921).

25. Macleod, D. B. Transactions of Faraday Society 19, 38 (1923).

26. Mills, O. S. British Journal of Applied Physics 4, 247 (1953).

27. NGPSA Engineering Data Book, 1966 edition.

28. Niederhauser, D. O., and F. E. Bartell. "Report of Progress -- Fundamental Research on Occurrence and Recovery of Petroleum," 1948-49. American Petroleum Institute, Baltimore, Md., 114 (1950).

29. Pennington, B. F., and E. W. Hough. Producers Monthly 29 (7), 4 (1965).

30. Quayle, O. R. Chemical Reviews 53, 439 (1953).

31. Rackett, H. G. S. M. Thesis, Massachusetts Institute of Technology, Cambridge, Massachusetts (1960).

32. Rackett, H. G. Private Communication.

33. Ramsay, W., and J. Shields. Philosophical Transactions 184, 647 (1893).

34. Reamer, H. H., B. H. Sage, and W. N. Lacey. Industrial and Engineering Chemistry 38, 986 (1946).

35. Reamer, H. H., B. H. Sage, and W. N. Lacey. Industrial and Engineering Chemistry 39, 77 (1947).

36. Reamer, H. H., B. H. Sage, and W. N. Lacey. Industrial and Engineering Chemistry 43, 1436 (1951).

37. Reilly, J., and W. N. Rae. Physico-Chemical Methods, 3rd. ed. Princeton, N. J.: D. Van Nostrand, 1939.

38. Reno, G. J., and D. L. Katz. Industrial and Engineering Chemistry 35, 1091 (1943).

39. Riedel, L. Chem.-Ing.-Tech. 26, 83 (1954).

40. Sage, B. H., and W. N. Lacey. Some Properties of the Lighter Hydrocarbons, Hydrogen Sulfide, and Carbon Dioxide. New York: American Petroleum Institute, 1955.

41. Savvina, Y. O., and A. S. Velikovskii. Journal of Physical Chemistry (USSR) 30, 1596 (1956).

42. Shipman, L. M., and J. P. Kohn. Journal of Chemical and Engineering Data 11 (2), 176 (1966).

43. Sprow, F. B., and J. M. Prausnitz. Transactions of Faraday Society 62, 1097 (1966).

44. Stauffer, C. E. Journal of Physical Chemistry 69, 1933 (1965).

45. Stegemeier, G. L. PhD Dissertation, University of Texas, Austin, Texas (1959).

46. Sugden, S. Journal of Chemical Society, 858 (1922).

47. Sugden, S. The Parachor and Valency. London: George Routledge and Sons, Ltd., 1930.

48. van der Waals, J. D. Zeitschrift fur Physikalische Chemie 13, 617 (1894).

49. Wark, I. W. Journal of Physical Chemistry 37, 623 (1933).

50. Warren, H. G. PhD Dissertation, Mississippi State University, State College, Mississippi (1965).

51. Weber, J. H. "Absorption Literature Survey," prepared for Natural Gas Processors' Association. September 3, 1964.

52. Weinaug, C. F., and D. L. Katz. Industrial and Engineering Chemistry 35, 239 (1943).

53. Wright, F. J. Journal of Applied Chemistry 11, 193 (1961).

54. Yarborough, L., and J. L. Vogel. Chemical Engineering Progress Symposium Series 63, No. 81, 1 (1967).

55. Yen, L. C., and S. S. Woods. A. I. Ch. E. Journal 12, 95 (1966).

APPENDIX A

CALCULATION OF ERRORS

CALCULATION OF ERRORS

The most probable value of error in interfacial tension as a result of uncertainties in experimentally measured quantities can be calculated by the calculus method described by Stegemeier (45). The equations for calculation of interfacial tension from pendant drop measurements are

$$\gamma = \frac{g\,\Delta\rho\,d_e^2}{H} \tag{34}$$

$$\frac{1}{H} = f(S) \tag{35}$$

$$S = \frac{d_s}{d_e}. \tag{36}$$

Error in interfacial tension can result from errors in the gravitational constant, density difference, equatorial diameter, and selected plane diameter.

Error in interfacial tension as a result of error in the gravitational constant is expressed as

$$\gamma_g = \left(\frac{\partial\gamma}{\partial g}\right)\delta_g = \left[\Delta\rho\left(\frac{1}{H}\right)d_e^2\right]\delta_g = \left(\frac{\gamma}{g}\right)\delta_g \tag{37}$$

where δ_g is the error in the gravitational constant.

Error in interfacial tension as a result of error in density difference is

$$\gamma_{\Delta\rho} = \left(\frac{\partial\gamma}{\partial\Delta\rho}\right)\delta_{\Delta\rho} = \left[g\left(\frac{1}{H}\,d_e^2\right)\right]\delta_{\Delta\rho} = \left(\frac{\gamma}{\Delta\rho}\right)\delta_{\Delta\rho} \tag{38}$$

Error in the equatorial diameter, d_e, appears in two terms of the interfacial tension equation

$$\gamma_{d_e} = \left(\frac{\partial \gamma}{\partial d_e}\right)\delta_{d_e} = \left[\frac{g\Delta\rho}{H} \cdot 2d_e + g\,\Delta\rho\, d_e^2 \frac{\partial(\frac{1}{H})}{\partial d_e}\right]\delta d_e . \quad (39)$$

From Equations (35) and (36),

$$\frac{\partial(\frac{1}{H})}{\partial d_e} = \frac{\partial(\frac{1}{H})}{\partial S}\frac{\partial S}{\partial d_e} = \frac{-d_s}{d_e^2}\frac{\partial(\frac{1}{H})}{\partial S}. \quad (40)$$

Stegemeier found from the tabulation of 1/H versus S data of Fordham (13) that

$$\frac{\partial(\frac{1}{H})}{\partial S} = -2.6444\ (\frac{1}{H})\frac{d_e}{d_s}. \quad (41)$$

Combining Equations (39), (40), and (41), the error in interfacial tension is

$$\gamma_{d_e} = 4.6444\ (\frac{\gamma}{d_e})\ \delta_{d_e}. \quad (42)$$

Error in the selected plane diameter, d_s, appears in the interfacial tension equation as

$$\gamma_{d_s} = g\,\Delta\rho\, d_e^2 \frac{\partial(\frac{1}{H})}{\partial d_s}. \quad (43)$$

From Equations (35) and (36),

$$\frac{\partial(\frac{1}{H})}{\partial d_s} = \frac{1}{d_e}\frac{\partial(\frac{1}{H})}{\partial S}. \quad (44)$$

Combining Equations (41), (43), and (44) gives the error in interfacial tension as a result of error in d_s as

$$\gamma_{d_s} = -2.6444 \left(\frac{\gamma}{d_s}\right) \delta_{d_s}. \tag{45}$$

The most probable value of the error in interfacial tension is expressed as

$$\Delta\gamma = \sqrt{\gamma_g^2 + \gamma_{\Delta\rho}^2 + \gamma_{d_e}^2 + \gamma_{d_s}^2}. \tag{46}$$

Substituting Equations (37), (38), (42), and (45) into Equation (46) gives

$$\Delta\gamma = \gamma \sqrt{\left(\frac{\delta_g}{g}\right)^2 + \left(\frac{\delta_{\Delta\rho}}{\Delta\rho}\right)^2 + \left(4.6444 \frac{\delta_{d_e}}{d_e}\right)^2 + \left(-2.6444 \frac{\delta_{d_s}}{d_s}\right)^2}. \tag{47}$$

A typical set of data for the methane-nonane system is

$$d_e = 0.2255 \text{ cm.}$$

$$d_s = 0.2002 \text{ cm.}$$

$$\Delta\rho = 0.6452 \text{ gm/cc.}$$

$$\gamma = 13.68 \text{ dyne/cm.}$$

Assuming the following uncertainties

$$\delta_g \doteq 0$$

$$\delta_{\Delta\rho} = 0.006$$

$$\delta_{d_e} = 0.001$$

$$\delta_{d_s} = 0.001,$$

the most probable value of error in interfacial tension from Equation (47) is

$$\Delta\gamma = 0.357.$$

Then

$$\gamma = 13.68 \pm 0.36 \text{ dynes/cm.}$$

APPENDIX B

LIQUID DENSITY CORRELATIONS

LIQUID DENSITY CORRELATIONS

Knowledge of the density of saturated liquid mixtures is required for many engineering design calculations and applications. For example, accurate values of liquid density are needed for the determination of viscosity and interfacial tension. Because liquid-phase densities are difficult to determine experimentally, a simple and general equation for predicting liquid-phase densities proves very useful. Few correlations for liquid mixture densities are available in the literature, and these range in complexity, degree of accuracy, and generality. The most commonly used methods are the Yen and Woods (55), Harmens (18), NGPA procedure (27), and the API recommended procedure (3).

Recently, Rackett (31) has reported a simple and general equation for the saturated liquid volume (or density) of pure substances

$$V_s/V_c = z_c^{[(1-T_r)^{2/7}]} . \qquad (48)$$

Rackett tested Equation (48) with pure-component literature data for 106 substances and found it to hold within experimental uncertainty for 93 of these substances.

The extension of the pure-component Rackett equation to mixtures merely requires the use of pseudo-critical properties. The mixture critical volume and compressibility factor are molal-average quantities

$$V_c = \Sigma\, x_i\, V_{c_i} \tag{49}$$

$$z_c = \Sigma\, x_i\, z_{c_i}. \tag{50}$$

The reduced temperature of the mixture can be determined from available mixture density data. Rackett showed from experimental data of binary systems that the critical temperature of a mixture of components from a homologous series (in particular, the paraffin hydrocarbons) is greater than the pseudo-critical temperature based on molal-average calculations

$$T_c > \Sigma\, x_i\, T_{c_i}. \tag{51}$$

Therefore, Rackett weighted the critical temperature of a binary mixture in favor of the heavier component as

$$T_c = \frac{\Sigma\, b_i\, x_i\, T_{c_i}}{\Sigma\, b_i\, x_i} \tag{52}$$

where $b = 1$ for the light component and $b > 1$ for the heavy component.

In order to determine the weighting factors for binary mixtures, Rackett used binary density data from the literature and calculated the best weighting factors for the heavy components from Equation (48) and Equation (52). These weighting factors were expressed graphically as a function of the difference of pure-component critical

temperatures for the binary systems as shown in Figure 18.

Summarizing, for binary mixtures, calculation of the liquid density requires selection of the weighting factor for the heavier component from Figure 18, calculation of the pseudo-critical properties according to Equations (49), (50), and (52), and substitution of these quantities into Equation (48).

Calculation of a mixture critical temperature for multicomponent systems is considerably more difficult than for binary systems. If the same weighting factor approach as in Equation (52) is used, weighting factors for each component in the mixture with every other component must be determined. Moreover, the individual b_i for a component to be used in Equation (52) must be calculated from some combination of the binary weighting factors for that component with every other component.

The problem of calculating the multicomponent critical temperature was solved by performing a matrix-type calculation (32) on the binary weighting factors. For example, for a ternary mixture, the individual weighting factors for the three components to be used in Equation (52) are calculated as

$$\begin{aligned} b_1 &= b_{1-1}^{X_1} \times b_{1-2}^{X_2} \times b_{1-3}^{X_3} \\ b_2 &= b_{2-1}^{X_1} \times b_{2-2}^{X_2} \times b_{2-3}^{X_3} \\ b_3 &= b_{3-1}^{X_1} \times b_{3-2}^{X_2} \times b_{3-2}^{X_3} . \end{aligned} \tag{53}$$

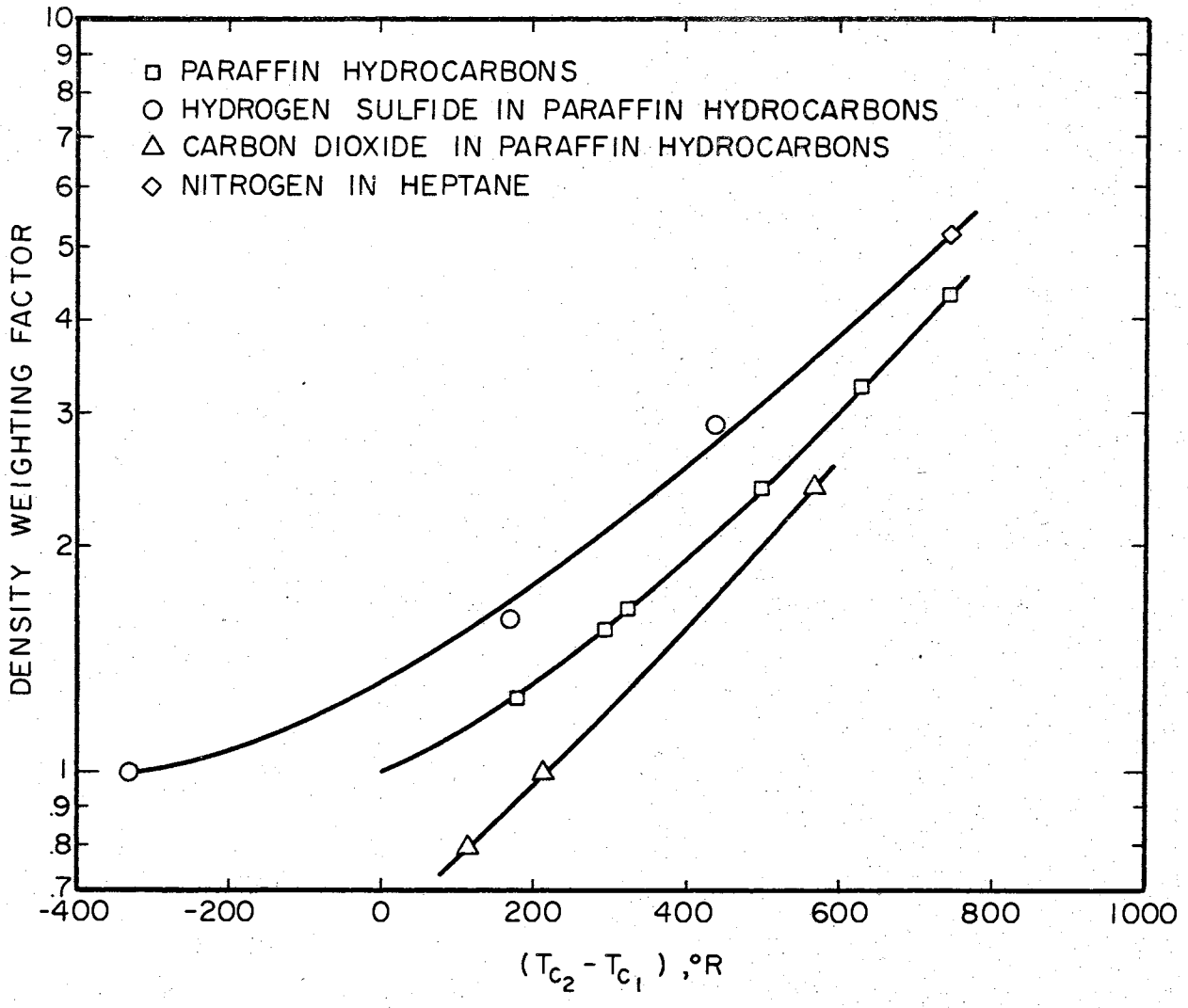

Figure 18. Density Weighting Factor

The b_{i-j} in Equation (53) represents the weighting factor for the binary mixture of components i and j. Each b_{i-j} with i = j is unity. Also, if component j represents a component that is heavier than component i, then b_{j-i} is greater than unity, and b_{i-j} is the reciprocal of b_{j-i}.

Therefore, for a multicomponent mixture, the Rackett method reduces to solution for the component weighting factors using binary weighting factors from Figure 18, substitution of the weighting factors into Equation (52) to calculate the mixture pseudo-critical temperature, and substitution of the pseudo-critical properties into Equation (48).

In seeking a reliable technique for predicting liquid-phase densities, the author investigated the Rackett method and the methods cited earlier. Table XVII and Figure 19 show the results of these methods compared with experimental data for the 100° F isotherm of the methane-pentane system. The Rackett method reproduces experimental data within experimental uncertainty, while results from the other procedures deviate significantly from experimental data. In view of the simplicity and accuracy of the Rackett method, this technique was applied to mixtures of hydrocarbons and non-hydrocarbons. Tables XVIII and XIX summarize the results for thirteen binary mixtures, one ternary system, and one nine-component mixture.

TABLE XVII

COMPARISON OF CALCULATED AND EXPERIMENTAL METHANE-PENTANE LIQUID DENSITY

P, psia	Mole Fraction Methane	Experimental Density	Calculated Saturated Liquid Density and Per Cent Error				
			Rackett	Harmens	NGPA	Yen-Woods	API
1000	.3077	.5436	.5424 -0.2	.5370 -1.2	.544 +0.1	.4959 -8.8	reference point
1250	.3748	.5248	.5232 -0.3	.5158 -1.7	.518 -1.3	.4628 -11.8	.514 -2.1
1500	.4390	.5033	.5022 -0.2	.4952 -1.6	.490 -2.6	.4240 -15.8	.477 -5.2
1750	.5041	.4772	.4773 0	.4681 -1.9	.453 -5.1	.3709 -22.3	.426 -10.8
2000	.5788	.4403	.4425 +0.5	.4310 -2.1	.395 -10.3	$T_r > 1$	off chart
2250	.6770	.3797	.3772 -0.7	.3663 -3.5	off chart	$T_r > 1$	off chart

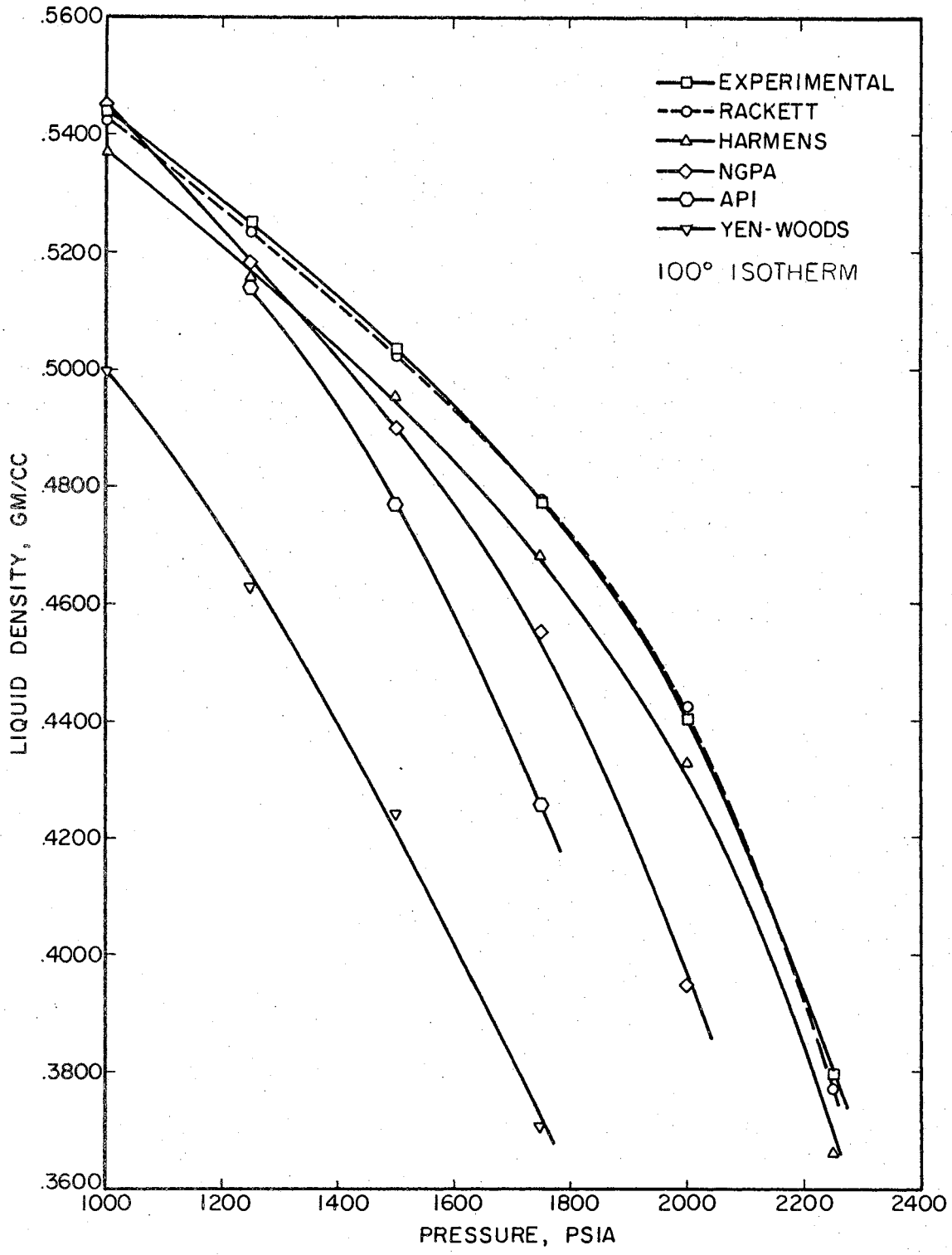

Figure 19. Calculated and Experimental Liquid Density for Methane-Pentane System

TABLE XVIII

COMPARISON OF RACKETT AND EXPERIMENTAL LIQUID DENSITY

System	No. of Points	Temp., °F	P, psia	Per Cent Error Max. Pos.	Per Cent Error Max. Neg.	Per Cent Error Avg. Abs.
C_1 -C_3	45	68-176	220-1176	1.70	2.04	1.11
-C_5	13	100-160	600-2250	0.50	2.00	0.69
-C_7	75	40-460	0-3000	1.84	2.82	0.57
-C_{10}	14	100-160	1500-5000	4.6	1.4	1.31
C_3 -C_{10}	61	40-460	0-802	2.35	1.24	0.88
C_4 -C_{10}	66	100-460	0-571	2.07	0.91	0.61
C_1 -C_4 -C_{10}	7	100	330-1150	0.9	0.9	0.66
H_2S-C_1	33	40-100	150-1750	-	1.32	0.72
-C_5	36	40-280	0-1700	0.76	3.29	0.92
-C_{10}	39	40-340	0-1400	2.43	1.61	1.14
CO_2 -C_3	26	40-130	80-600	2.63	2.32	0.92
-C_4	32	100-220	50-700	2.69	0.92	0.59
-C_{10}	79	40-460	0-2250	10.56	3.38	1.35
N_2 -C_7	28	90-360	1000-10,000	2.71	10.62	3.09

TABLE XIX

COMPARISON OF RACKETT AND EXPERIMENTAL DENSITY
FOR NINE-COMPONENT SYSTEM

Component	Mole Fraction	T, °F	P, psig	Liquid Density		Per Cent Error
				Expt'l.	Calculated-Rackett	
CO_2	.0506	75	340	.5127	.5125	-0.04
C_1	.0110					
C_2	.4033	100	445	.4888	.4893	+0.10
C_3	.2868					
iC_4	.0835	125	540	.4640	.4633	-0.16
nC_4	.0659					
iC_5	.0137					
nC_5	.0148					
C_7^+	.0704					

APPENDIX C

DATA USED FOR CORRELATION ANALYSIS

TABLE XX

FERGUSON EQUATION CONSTANTS

Component	γ_o	n	Source of Data
Methane	39.05	1.221	(43)
Propane	49.90	1.20	(45)
Butane	52.50	1.22	(45)
Pentane	52.90	1.22	(3)
Heptane	47.27	1.099	(50)
Nonane	51.60	1.22	(3)
Decane	51.60	1.22	(3)
Ethylene	51.80	1.25	(24)
Nitrogen	28.42	1.232	(43)

TABLE XXI

EXCESS INTERFACIAL TENSION FROM METHANE-PROPANE DATA OF WEINAUG AND KATZ (52)

T, °F	P, psia	Mole Fraction Methane	Interfacial Tension	T_r	γ^E (Equation 33)
86	220	.024	5.91	.825	-0.203
86	311	.059	5.25	.834	-0.439
86	419	.100	4.43	.845	-0.755
86	510	.136	3.83	.856	-0.898
86	583	.166	3.37	.865	-0.969
86	744	.229	2.34	.885	-1.168
86	808	.255	2.14	.894	-1.018
86	858	.279	1.73	.903	-1.099
86	948	.314	1.30	.916	-1.046
86	982	.336	1.11	.925	-0.933
86	1039	.355	0.82	.933	-0.958
86	1230	.452	0.19	.978	-0.267
113	348	.046	3.78	.872	-0.407
113	518	.110	2.79	.890	-0.637
113	619	.149	2.30	.902	-0.655
113	623	.151	2.23	.903	-0.703
113	692	.178	1.87	.911	-0.730
113	728	.192	1.70	.916	-0.727
113	733	.194	1.68	.917	-0.725
113	821	.230	1.30	.929	-0.659
113	872	.250	1.06	.936	-0.650
113	893	.258	0.97	.939	-0.642
113	982	.297	0.64	.954	-0.487
149	435	.032	2.05	.923	-0.238
149	480	.047	1.87	.927	-0.255
149	615	.096	1.28	.942	-0.327
149	718	.136	0.87	.954	-0.313
149	830	.184	0.54	.971	-0.147
149	935	.233	0.22	.989	0.004

TABLE XXII

EXCESS INTERFACIAL TENSION FROM METHANE-BUTANE DATA OF PENNINGTON (29)

T, °F	P, psia	Mole Fraction Methane	Interfacial Tension	T_r	γ^E (Equation 33)
100	1300	.4131	2.18	.818	-3.70
100	1400	.4465	1.64	.829	-3.75
100	1500	.4799	1.15	.841	-3.72
130	1400	.4193	1.16	.864	-2.95
130	1500	.4521	0.765	.876	-2.88
160	1400	.3978	0.71	.900	-2.13
160	1500	.4329	0.428	.913	-1.95

TABLE XXIII

EXCESS INTERFACIAL TENSION FROM METHANE-PENTANE DATA OF STEGEMEIER (45)

T, °F	P, psia	Mole Fraction Methane	Interfacial Tension	T_r	γ^E (Equation 33)
100	1000	.3077	6.16	.731	-3.623
100	1250	.3748	4.60	.753	-4.056
100	1500	.4390	3.22	.778	-4.257
100	1750	.5041	2.01	.807	-4.163
100	2000	.5788	1.01	.848	-3.497
100	2250	.6770	0.265	.919	-1.749
160	600	.1655	6.65	.769	-1.824
160	800	.2212	5.52	.783	-2.186
160	1000	.2743	4.49	.799	-2.438
160	1250	.3381	3.45	.820	-2.489
160	1500	.4002	2.35	.844	-2.554
160	1750	.4671	1.37	.874	-2.330
160	2000	.5460	0.56	.918	-1.597
160	2250	.6654	0.059	.930	-1.628

TABLE XXIV

EXCESS INTERFACIAL TENSION FROM METHANE-HEPTANE DATA OF WARREN (50)

T, °F	P, psia	Mole Fraction Methane	Interfacial Tension	T_r	γ^E (Equation 33)
100	200	.064	16.30	.583	-1.475
100	400	.124	14.50	.591	-2.617
100	600	.181	12.90	.600	-3.557
100	800	.234	10.95	.609	-4.857
100	1000	.284	9.85	.619	-5.30

TABLE XXV

EXCESS INTERFACIAL TENSION FROM ETHYLENE-HEPTANE DATA OF WARREN (50)

T, °F	P, psia	Mole Fraction Ethylene	Interfacial Tension	T_r	γ^E (Equation 33)
100	200	.225	13.94	.615	-2.419
100	400	.420	9.75	.665	-4.046
100	600	.586	5.96	.725	-4.819
160	200	.161	12.29	.667	-1.669
160	400	.309	9.26	.702	-2.903
160	600	.436	6.59	.741	-3.628

TABLE XXVI

EXCESS INTERFACIAL TENSION FROM NITROGEN-HEPTANE DATA OF RENO AND KATZ (38)

T, °F	P, psia	Mole Fraction Nitrogen	Interfacial Tension	T_r	γ^E (Equation 33)
77	214	.0193	18.71	.553	-0.634
77	514	.0455	17.16	.556	-1.787
77	1014	.0856	14.90	.561	-3.475
131	214	.0211	16.12	.609	-0.550
131	514	.0494	14.44	.613	-1.831
131	1016	.0930	12.41	.618	-3.287
185	214	.0229	13.31	.665	-0.723
185	513	.0532	12.04	.669	-1.630
185	1001	.1002	10.55	.675	-2.522

TABLE XXVII

EXCESS INTERFACIAL TENSION FROM METHANE-NONANE DATA OF THIS STUDY

T, °F	P, psia	Mole Fraction Methane	Interfacial Tension	T_r	γ^E (Equation 33)
76	75	.0254	21.77	.501	-0.168
76	150	.0509	20.58	.504	-1.103
76	300	.0986	18.93	.508	-2.262
30	15	.0054	24.37	.457	-0.105
30	150	.0540	22.95	.461	-1.027
30	300	.1069	19.27	.465	-4.148
30	600	.2023	16.28	.475	-6.072
30	900	.2838	13.68	.485	-7.691
30	1175	.3515	10.48	.495	-10.008
30	1315	.3801	9.30	.500	-10.791
30	1475	.4087	8.26	.505	-11.421
-10	140	.0687	25.05	.424	-0.827
-10	310	.1288	21.79	.429	-3.431
-10	598	.2381	15.91	.440	-8.047
-10	890	.3302	12.17	.452	-10.625
-10	1190	.4051	9.27	.464	-12.486
-30	147	.0796	24.45	.406	-2.346
-30	285	.1458	21.73	.412	-4.333
-30	590	.2627	16.38	.423	-8.303
-30	1025	.3994	10.41	.442	-12.453

TABLE XXVIII

EXCESS INTERFACIAL TENSION FROM METHANE-DECANE DATA OF STEGEIMEIER (45)

T, °F	P, psia	Mole Fraction Methane	Interfacial Tension	T_r	γ^E (Equation 33)
100	1500	.3637	9.76	.532	-8.853
100	2000	.4469	7.35	.544	-10.280
100	2500	.5183	5.67	.557	-11.006
100	3000	.5827	3.66	.573	-12.021
100	3500	.6370	2.40	.590	-12.304
100	4000	.6870	1.43	.609	-12.209
100	5000	.8064	0.163	.690	-9.774
160	1500	.3429	9.77	.586	-6.335
160	2000	.4234	7.52	.598	-7.683
160	2500	.4943	5.50	.612	-8.805
160	3000	.5593	3.75	.628	-9.605
160	3500	.6202	2.41	.647	-9.900
160	4000	.6796	1.38	.671	-9.701
160	5000	.8240	0.062	.785	-6.266

TABLE XXIX

EXCESS INTERFACIAL TENSION FROM METHANE-BUTANE-DECANE DATA OF THIS STUDY

T, °F	P, psia	Mole Fraction Methane	Interfacial Tension	T_r	γ^E (Equation 33)
40	290	.10	18.24	.469	-5.090
40	555	.20	14.65	.477	-7.699
40	1000	.317	11.55	.488	-9.568
100	325	.10	16.79	.523	-3.658
100	685	.20	13.95	.532	-5.562
100	1145	.30	10.91	.542	-7.579
100	370	.10	14.69	.559	-4.014
100	730	.20	12.68	.569	-5.025
100	1120	.30	9.93	.582	-6.677
100	332	.10	13.68	.598	-3.071
100	671	.20	11.72	.610	-3.977
100	1057	.30	9.54	.626	-5.005

APPENDIX D

CRITICAL CONSTANTS USED FOR CORRELATIONS

TABLE XXX

CRITICAL CONSTANTS

Component	Z_c	T_c, °R	V_c, ml/g mole
Methane	.289	344	99
Ethane	.278	550	144.7
Propane	.276	666	200
i-Butane	.275	735	255.5
n-Butane	.273	765.5	255.5
i-Pentane	.270	830	310.5
n-Pentane	.268	845	311
n-Heptane	.260	973	426
n-Decane	.251	1115	613
Nitrogen	.289	227	89.4
Carbon dioxide	.272	548	93.4
Hydrogen sulfide	.284	672.5	97.7
Ethylene	.282	519	131

APPENDIX E

DENSITY AND DROP MEASUREMENT DATA FOR EXPERIMENTAL RUNS

TABLE XXXI

DENSITY AND DROP MEASUREMENT DATA FOR EXPERIMENTAL METHANE-NONANE DATA

Y	d_n	d_s	d_e	d_L	d_v
22.71	.4915	.5968	.6992	.7144	.00115
22.74	.4909	.5963	.6987	.7144	.00115
22.79	.4920	.5955	.6992	.7144	.00115
22.82	.4933	.5930	.6985	.7144	.00115
22.74	.4898	.5947	.6970	.7144	.00115
21.94	.4983	.5916	.6963	.7091	.00348
21.79	.4983	.5903	.6944	.7091	.00348
21.50	.5020	.5900	.6944	.7091	.00348
21.87	.4958	.5841	.5841	.7091	.00348
20.63	.4952	.5831	.6809	.7065	.0067
20.62	.4976	.5844	.6831	.7065	.0067
20.50	.4970	.5850	.6823	.7065	.0067
20.58	.4968	.5843	.6823	.7065	.0067
18.93	.4949	.5743	.6650	.7013	.0136
25.15	.4643	.5626	.6704	.7344	.00113
25.29	.4630	.5617	.6702	.7344	.00113
25.30	.4600	.5603	.6670	.7344	.00113
24.66	.4698	.5640	.6718	.7347	.00073
24.07	.4618	.5575	.6590	.7347	.00073
23.47	.4669	.5553	.6595	.7293	.0076
22.44	.4728	.5610	.6605	.7293	.0076
19.27	.4690	.5331	.6215	.7224	.0155
16.33	.4573	.5157	.5878	.7086	.0327
16.23	.4564	.5177	.5878	.7086	.0327
13.68	.4650	.5077	.5710	.6957	.0505
13.69	.4603	.4900	.5572	.6957	.0505
10.53	.4623	.4871	.5316	.6829	.0707
10.56	.4590	.4830	.5278	.6829	.0707
10.36	.4558	.4754	.5193	.6829	.0707
9.22	.4595	.4679	.5065	.6770	.0815
9.13	.4716	.4920	.5261	.6770	.0815
9.36	.4675	.4709	.5137	.6770	.0815
9.48	.4623	.4690	.5115	.6770	.0815
8.33	.4537	.4554	.4885	.6722	.0925
8.24	.4516	.4523	.4846	.6722	.0925
8.20	.4556	.4594	.4903	.6722	.0925
25.32	.4950	.6161	.7261	.74475	.00814
24.94	.4752	.5745	.6833	.74475	.00814
24.89	.4745	.5781	.6850	.74475	.00814
21.15	.4750	.5631	.6555	.7361	.0179

TABLE XXXI (Continued)

γ	d_n	d_s	d_e	d_L	d_v
22.79	.4585	.5573	.6522	.7361	.0179
21.46	.4902	.5768	.6757	.7361	.0179
21.74	.4863	.5648	.6672	.7361	.0179
16.08	.4960	.5443	.6201	.7203	.0368
15.31	.4938	.5466	.6180	.7203	.0368
15.92	.4925	.5467	.6225	.7203	.0368
16.32	.4919	.5440	.6237	.7203	.0368
12.27	.4932	.5275	.5845	.7042	.0596
12.02	.4916	.5281	.5815	.7042	.0596
12.32	.4905	.5241	.5815	.7042	.0596
12.06	.4950	.5315	.5858	.7042	.0596
9.28	.4938	.5075	.5470	.6886	.0868
9.26	.4941	.5090	.5478	.6886	.0868
24.60	.5255	.6365	.7531	.7502	.00854
24.31	.5249	.6382	.7520	.7520	.00854
21.10	.5220	.6164	.7172	.7417	.01785
21.67	.5298	.6212	.7291	.7417	.01785
22.42	.5111	.6052	.7125	.7417	.01785
15.99	.5037	.5507	.6315	.7240	.03927
15.99	.4938	.5538	.6282	.7240	.03927
17.17	.4779	.5452	.6234	.7240	.03927
10.27	.5191	.5030	.5655	.6980	.0828
10.41	.5167	.5202	.5768	.6980	.0828
10.56	.5224	.5496	.6000	.6980	.0828
10.40	.5156	.5288	.5817	.6980	.0828

Note: d_n is magnified diameter of drop needle.

TABLE XXXII

DENSITY AND DROP MEASUREMENT DATA FOR EXPERIMENTAL BUTANE-DECANE AND METHANE-BUTANE-DECANE DATA

γ	d_n	d_s	d_e	d_L	d_v
20.08	3.911	4.455	5.243	.70473	.00142
20.05	3.900	4.462	5.240	.70473	.00142
20.19	3.839	4.353	5.139	.70473	.00142
19.90	3.858	4.390	5.159	.70473	.00142
16.82	3.945	4.376	5.066	.67461	.00387
16.98	3.954	4.275	5.014	.67461	.00387
16.96	3.951	4.358	5.066	.67461	.00387
15.51	3.648	3.904	4.559	.64379	.00553
15.96	3.658	3.843	4.503	.64379	.00553
21.35	.5200	.6045	.7093	.7262	.00062
21.21	.5073	.5924	.6933	.7262	.00062
21.40	.5216	.5955	.7051	.7262	.00062
17.02	3.899	4.374	5.049	.6885	.01593
16.99	3.872	4.380	5.036	.6885	.01593
16.36	4.066	4.343	5.137	.6885	.01593
13.85	4.033	4.400	4.972	.67280	.03386
14.05	4.031	4.363	4.962	.67280	.03386
10.95	4.026	4.305	4.723	.66172	.05843
10.79	4.001	4.210	4.636	.66172	.05843
11.00	4.034	4.190	4.659	.66172	.05843
14.47	3.927	4.388	4.948	.66349	.02111
14.70	4.094	4.425	5.079	.66349	.02111
14.70	4.109	4.493	5.131	.66349	.02111
14.51	3.991	4.365	4.971	.66349	.02111
15.08	3.931	4.289	4.930	.66349	.02111
12.87	4.009	4.242	4.833	.64804	.04036
12.61	3.998	4.249	4.810	.64804	.04036
12.71	3.983	4.144	4.742	.64804	.04036
12.79	3.889	4.226	4.753	.64804	.04036
12.42	3.897	4.113	4.655	.64804	.04036
9.95	3.838	4.062	4.448	.62815	.06361
9.79	3.842	4.067	4.437	.62815	.06361
10.05	3.826	4.031	4.433	.62815	.06361
13.91	3.987	4.430	5.023	.62927	.02060
13.44	4.037	4.460	5.032	.62927	.02060
13.33	4.011	4.433	4.992	.62927	.02060
14.02	4.044	4.412	5.051	.62927	.02060
11.81	4.097	4.239	4.849	.61166	.03959
11.57	4.036	4.252	4.805	.61166	.03959
11.78	4.044	4.230	4.814	.61166	.03959

TABLE XXXII (Continued)

γ	d_n	d_s	d_e	d_L	d_v
9.36	3.952	4.165	4.578	.59060	.06430
9.60	3.904	4.135	4.560	.59060	.06430
9.44	3.924	4.159	4.568	.59060	.06430
9.75	3.934	4.173	4.614	.59060	.06430
18.38	.5182	.5940	.6852	.7114	.01366
18.22	.5099	.5926	.6783	.7114	.01366
18.11	.5048	.5793	.6658	.7114	.01366
14.66	.5037	.5506	.6238	.6956	.03014
14.45	.5120	.5559	.6297	.6956	.03014
14.71	.5036	.5531	.6258	.6956	.03014
14.58	.5040	.5496	.6226	.6956	.03014
14.87	.5088	.5543	.6308	.6956	.03014
11.74	.4998	.5235	.5860	.6725	.05881
11.36	.5004	.5306	.5867	.6725	.05881
11.55	.5004	.5290	.5880	.6725	.05881

Note: d_n is magnified diameter of drop needle
diameter measurements greater than 1.0 are in inches
diameter measurements less than 1.0 are in centimeters

VITA

James Richard Deam

Candidate for the Degree of

Doctor of Philosophy

Thesis: INTERFACIAL TENSION IN HYDROCARBON SYSTEMS

Major Field: Chemical Engineering

Biographical:

Personal Data: Born in Springfield, Ohio, January 9, 1942, to Richard H. and Mary E. Deam. Married to Linda Kay Roberson, May 21, 1966.

Education: Attended elementary school in Springfield, Ohio; graduated from Springfield High School, Springfield, Ohio; received Degree of Bachelor of Science in Chemical Engineering from University of Cincinnati, Cincinnati, Ohio, June 14, 1964; received Degree of Master of Science from Oklahoma State University in May, 1966; completed requirements for Degree of Doctor of Philosophy in May, 1969.

Membership in Scholarly or Professional Societies: Tau Beta Pi, Omega Chi Epsilon, Phi Lambda Upsilon, Sigma Xi, Alpha Chi Sigma, Affiliate Member of the American Institute of Chemical Engineers.

Professional Experience: Employed by International Harvester Company, Springfield, Ohio, as part of co-operative engineering program at the University of Cincinnati from June, 1960, to December, 1963; employed as a Summer Student by Battelle Memorial Institute, Columbus, Ohio, during the summer of 1964; employed by Houston Research Laboratory of Shell Oil Company as a Research Engineer during the summer of 1966.